Energy 174 (2019) 292–309

Contents lists available at ScienceDirect

Energy

journal homepage: www.elsevier.com/locate/energy

Review

Efficiency in RF energy harvesting systems: A comprehensive review

Mustafa Cansiz [a], Dogay Altinel [b, c, *], Gunes Karabulut Kurt [c]

[a] Department of Electrical and Electronics Engineering, Dicle University, Diyarbakir, Turkey
[b] Department of Electrical and Electronics Engineering, Istanbul Medeniyet University, Istanbul, Turkey
[c] Department of Electronics and Communication Engineering, Istanbul Technical University, Istanbul, Turkey

ARTICLE INFO

Article history:
Received 18 August 2018
Received in revised form
8 February 2019
Accepted 13 February 2019
Available online 18 February 2019

Keywords:
Energy harvesting
RF energy harvesting
Efficiency
Conversion efficiency
Impedance matching efficiency

ABSTRACT

One of the most important research areas searches for new sources of energy and for the highest efficiency from existing energy sources. Radio frequency (RF) energy harvesting is a promising alternative to obtain energy for wireless devices directly from RF energy sources in the environment. In this paper, we provide a broad overview of the main blocks of RF energy harvesting systems, which are the wireless transmission medium, the antenna and impedance matching circuit, the rectifier, the voltage multiplier, and the energy storage device or load. The characteristics of these blocks directly affect the performance of an RF energy harvesting system. We mainly focus on the ratio of output and input powers at each block, named as the conversion efficiency and the impedance matching efficiency, which determines the overall efficiency of system. We present detailed information about the system parameters. Thus, we characterize an RF energy harvesting system, which makes the design of system possible to obtain the maximum efficiency and correspondingly the maximum output power, providing the necessary insight about the design of RF energy harvesting systems.

Contents

* Corresponding author. Department of Electrical and Electronics Engineering, Istanbul Medeniyet University, Istanbul, Turkey.
E-mail address: dogay.altinel@medeniyet.edu.tr (D. Altinel).

https://doi.org/10.1016/j.energy.2019.02.100
0360-5442/

1. Introduction

Wireless devices need energy as their primary resource to maintain their operations. However, the capacity of batteries, commonly used to power wireless devices, is limited. Their lifespan is also limited. Hence, a sustainable operation cannot be achieved for wireless devices and networks. In order to overcome this challenge, energy harvesting from existing energy sources in their surroundings has emerged as a promising technology. There are various energy sources such as solar, thermal gradients, mechanical vibrations and electromagnetic waves in the ambient environment [1]. For energy harvesting, the power density of these sources is very important. Among these energy sources, solar energy has the highest power density and is considered to be the most utilized energy source [2]. During daytime, the average power density of solar energy is around 100 mW/cm^2 [3], however clouds can reduce this output and at night the power density drops to zero. Furthermore, solar panels occupy a large area. Electric potential is obtained when thermoelectric materials are heated [4]. They can operate in reverse by applying an electric potential to produce heat. At room temperature, the power density of thermal energy is approximately between 20 μW/cm^2 and 60 μW/cm^2 when human body is used as a thermal source [5]. Piezoelectric materials generate electrical power from mechanical vibrations, motions or noise [6]. Due to high voltage and low current, this type of energy source has low conversion efficiency and needs a voltage regulator for preventing circuit from voltage overshoots [7]. The power density of piezoelectric energy depends on the characteristics of motion but typical a value is about 250 μW/cm^3 [8].

In the ambient environments, radio frequency (RF) energy has the lowest power density when compared to the aforementioned energy sources. The power density of RF energy varies between 0.2 nW/cm^2 and 1 μW/cm^2 [9,10]. On the other hand, RF energy can be obtained from electromagnetic waves over a vast area. Electromagnetic waves of RF energy sources radiating in different frequency bands are ubiquitous and available even in inaccessible places, and hence, it is possible to extract energy from this wide area. Moreover, RF energy harvesting can be used together with information transfer in communication systems such as wireless powered communication (WPC) and simultaneous wireless information and power transfer (SWIPT) systems [11,12]. Additionally, the use of low-power wireless devices has been increasing. Because of these reasons, RF energy harvesting attracts great attention, and considerable improvements have been observed in RF energy harvesting technology in the recent years [13–15]. RF energy harvesters provide a viable energy source for applications such as wireless sensor networks (WSNs) and internet of things. These sensors are used in many fields including agriculture, defense, energy management, building automation, security, industrial monitoring, health monitoring, environment monitoring, data center and smart grid. In addition to that, low power consumer electronics (e.g. remote controllers, keyboards, headsets and low power displays) emerge as another convenient practical application area of RF energy harvesting. In this context, RF energy harvesting applications can be exemplified here. P2110 Powerharvester module from Powercast Company is a commercial product that enables efficient energy harvesting in the frequency range from 902 MHz to 928 MHz [16]. Thanks to the RF energy harvester development kits, AA or AAA size batteries can be charged and light emitting diodes (LEDs) can be lit wirelessly. In Ref. [17], wireless sensors were distributed in a field of agricultural crops in order to detect and monitor pests. Similarly, these sensors can also be used to collect data such as temperature, mineral content and humidity of soil. In Ref. [18], smart meter and LCD display were connected to the wireless energy harvester. A folded dipole antenna was designed, fabricated and then attached to the energy harvester. In that study, it was shown that the smart meter and LCD display was successfully powered by the wireless energy harvester.

An RF energy harvesting circuit usually consists of an antenna, an impedance matching circuit, a rectifier, a voltage multiplier, and an energy storage device or load, as will be reviewed in this paper. In an RF energy harvesting system, first, the transmitted RF signal propagating through wireless transmission medium is captured by a single antenna or multiple antennas in the far-field region. The impedance matching circuit is used to provide the maximum power transfer. Then, the rectifier converts RF power in direct current (DC). The output voltage of the rectifier is usually very low to drive a wireless device. Therefore, a voltage multiplier is used to increase the DC voltage level. Finally, the harvested energy can be stored into an energy storage device, such as a rechargeable battery and a supercapacitor, or can be directly connected to the load. Note that an RF energy harvesting system targets harvesting RF signal energy in the far-field region of antenna, unlike inductive coupling and magnetic resonance coupling in the near-field region of antenna.

In this paper, we aim to evaluate the performance of an RF energy harvesting system, which can be determined by using the overall efficiency parameter. The overall efficiency ($\eta_{overall}$) of RF energy harvesting system can be defined as

$$\eta_{overall} = \frac{\text{DC output power}}{\text{RF input power}}. \quad (1)$$

Here, the overall efficiency is the ratio between the DC output power delivered to the load and the RF input power coming into the system. It depends on many parameters such as transmit power, frequency band, operation voltage, and load impedance. It also enables the harvested power to be expressed in terms of the input power.

The block diagram of an RF energy harvesting system is shown in Fig. 1, including the input-output powers and efficiencies of the blocks. The blocks are transmitter, wireless transmission medium, antenna and matching circuit, rectifier, voltage multiplier, and energy storage device or load. Each block of an RF energy harvesting system has an impact on the overall efficiency. The efficiencies of each block can be combined into an overall efficiency, and the overall efficiency of RF energy harvesting system is formulated as

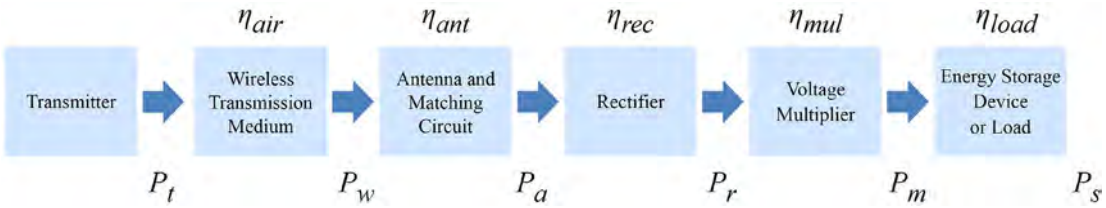

Fig. 1. Block diagram of an RF energy harvesting system with input-output powers and efficiencies. The efficiency parameters of these blocks constitute the overall efficiency, $\eta_{overall} = \eta_{air}\ \eta_{ant}\ \eta_{rec}\ \eta_{mul}\ \eta_{load}$.

$$\eta_{overall} = \frac{P_w}{P_t}\ \frac{P_a}{P_w}\ \frac{P_r}{P_a}\ \frac{P_m}{P_r}\ \frac{P_s}{P_m}, \tag{2}$$

and it can also be written as

$$\eta_{overall} = \eta_{air}\ \eta_{ant}\ \eta_{rec}\ \eta_{mul}\ \eta_{load}, \tag{3}$$

where the variables in the equations above are defined in Table 1.

Based on this approach, the overall efficiency of the system is expressed in terms of power and efficiency of each block. In this paper, each block will be examined in detail, and the efficiency of each block will be expressed separately in terms of the conversion efficiency and the impedance matching efficiency in the following sections. The remainder of this paper is organized as follows. Section 2 presents the wireless transmission medium including frequency bands and regions around an antenna. In Section 3, some antenna designs and matching circuits are explained. Section 4 and Section 5 provide the design and implementation of rectifier and voltage multiplier, respectively. In Section 6, energy storage types and loads are presented. Section 7 presents power management in energy harvesting systems. In Section 8, the efficiency of RF energy harvesting circuit is explained in detail. Conclusions are presented in Section 9.

2. Wireless transmission medium

In this section, we explain the wireless transmission medium block in an RF energy harvesting system by including the corresponding aspects of the transmitter that forms the input part of wireless transmission medium. We divide this section into three subsections as frequency bands, near-field and far-field regions, and efficiency of the wireless transmission medium.

2.1. Frequency bands

An RF energy harvesting system requires an RF signal source that radiates in the range between 3 kHz and 300 GHz of frequency spectrum. The range of RF spectrum is divided into various frequency bands such as very high frequency (VHF), ultra high frequency (UHF), super high frequency (SHF), or extremely high frequency (EHF) bands. In the ambient environment, transmitters radiating in the RF bands such as Television (TV), Frequency Modulation (FM), Global System for Mobile Communications (GSM), Universal Mobile Telecommunications System (UMTS), Long Term Evolution (LTE), and Wireless Fidelity (Wi-Fi) signals can be used as RF signal sources of RF energy harvesting systems. The output powers of transmitters directly affect the power level transferred to the harvesting antenna through the wireless transmission medium. The sufficient amount of transmitted power above the sensitivity threshold makes it possible to harvest energy in the RF energy harvesting systems and to operate wireless devices with the harvested energy. However, there are various restrictions on the output powers of transmitters. The maximum output powers have to comply with regulations. Restriction levels for the maximum output powers are recommended by some international organisations like Federal Communications Commission (FCC) [19], Institute of Electrical and Electronics Engineers (IEEE) [20] and International Commission on Non-Ionizing Radiation Protection (ICNIRP) [21] in order to protect human against the potential adverse health effects of non-ionizing electromagnetic fields.

Some common frequency bands and their ranges are listed in Table 2. Transmission from mobile phone to base station corresponds to the uplink channel. Likewise, transmission from base station to mobile phone constitutes the downlink channel. Since the uplink and downlink frequency bands may be different in frequency division duplexing, they can be utilized in RF energy harvesting separately as depicted in the table. Broadcast control channel (BCCH) in GSM technology and primary synchronization channel (P-SCH) in UMTS technology broadcast continuously but other traffic channels are activated when there are user requests in their mobile communication networks. Therefore, power levels of some bands such as GSM900, GSM1800, UMTS, LTE and Wi-Fi depend on user traffic densities. In other words, the higher the number of users in active mode, the higher the power levels in the environment. On the other hand, FM and TV transmitters broadcast continuously. FM systems broadcast in VHF band, TV systems

Table 1
Variables.

Symbol	Description
P_t	Transmitted power
P_w	Output power of wireless transmission medium
P_a	Output power of antenna and matching circuit
P_r	Output power of rectifier
P_m	Output power of voltage multiplier
P_s	Power used to store energy by energy storage device or power consumed by load
η_{air}	Efficiency of wireless transmission medium
η_{ant}	Efficiency of antenna and matching circuit
η_{rec}	Efficiency of rectifier
η_{mul}	Efficiency of voltage multiplier
η_{load}	Efficiency of energy storage device or load

Table 2
Frequency bands and ranges.

Frequency Band	Frequency Range (MHz)
VHF	30–300
FM	87.5–108
UHF	300–3000
TV	470–862
GSM900 UL	890–915
GSM900 DL	935–960
GSM1800 UL	1710–1785
GSM1800 DL	1805–1880
UMTS UL	1920–1980
UMTS DL	2110–2170
LTE UL	791-821, 880–915, 1710–1785, 1920–1980, 2500-2570
LTE DL	832-862, 925–960, 1805–1880, 2110–2170, 2620-2690
Wi-Fi	2400–2483.5
ISM	433, 915, 2450, 5800

UL: Uplink, DL: Downlink.

broadcast in both VHF and UHF bands, and digital mobile communication systems benefit from UHF band. Especially, VHF and UHF TV bands are the most suitable bands for RF energy harvesting because they propagate with relatively higher power levels.

2.2. Near-field and far-field regions

Antenna is used as the main front-end component in the RF energy harvester circuits. An antenna is a transducer for radiating or receiving electromagnetic waves, which is called as transmitting or receiving antenna, respectively. Here, in order to give insights about the radiation of RF power in the wireless transmission medium, we explain the field around an antenna of the transmitter of RF energy harvesting system as a transmitting antenna. As shown in Fig. 2, the field around an antenna of the transmitter is divided into three regions: reactive near-field, radiating near-field (Fresnel), and far-field (Fraunhofer) [22]. Here, R_1 and R_2 are the distances from source (antenna) for reactive near-field region and radiating near-field region, respectively. R_1 and R_2 distances can be expressed as

$$R_1 = 0.62\sqrt{\frac{D^3}{\lambda}}, \quad R_2 = \frac{2D^2}{\lambda}, \tag{4}$$

where λ is the wavelength of RF signal, and D is the largest dimension of the antenna. The other region (the distance larger than R_2) is the far-field region.

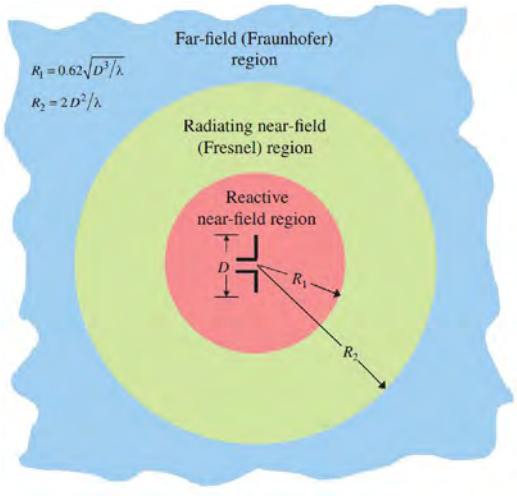

Fig. 2. Near-field and far-field regions around an antenna [22].

In the near-field region, inductive coupling and magnetic resonance coupling are used for power transfer. As an example, conversion efficiency above 77% at the frequency of 6 MHz [23] was obtained utilizing inductive coupling system for transmitting power in the near-field region. Moreover, wireless power transfer of 60 W via strongly coupled magnetic resonances with approximately 40% conversion efficiency over 2 m was experimentally demonstrated [24]. Radio frequency identification (RFID) is a good example for the system operating in both the near-field region and the far-field region. In terms of frequency range, passive RFID systems can be split into two groups: high frequency and ultra-high frequency RFID systems. High frequency RFID system can operate from a few centimeters up to a meter in the near-field region [25,26], whereas in the far-field region, ultra-high frequency RFID system works in larger range. The conversion efficiency of RF power transfer in the near-field region is higher than in the far-field region [23,24,27]. In the far-field region, although the power density value decreases as the distance from the source increases, there is a large area to extract energy from the environment. Moreover, sometimes the energy harvesting system must be far away from the source. In this paper, we mainly focus on the efficiency in the far-field region.

2.3. Efficiency of wireless transmission medium

Air is the wireless transmission medium between the transmitting and harvesting antennas in free space. The receiving antenna is the harvesting antenna for RF energy. The efficiency (η_{air}) can be formulated as the ratio of the wireless transmission medium output power to the transmitted power as

$$\eta_{air} = \frac{P_w}{P_t}. \tag{5}$$

For given the transmitted power, we need to express the wireless transmission medium. Firstly, we define the power density at the front end of the antenna. The power density of incident RF signal (S) is expressed by the transmitted power, the antenna gain, and the spherical surface as

$$S = \frac{\text{EIRP}}{4\pi r^2} = \frac{P_t G_t}{4\pi r^2}, \tag{6}$$

where EIRP is the effective isotropic radiated power, which is formulated as EIRP $= P_t G_t$. Here, G_t is the transmitting antenna gain. r is the distance from the transmitting antenna to the harvesting antenna.

In order to maximize the power density in air interface, some improvements may be suggested based on equation (6). Firstly, the transmitted power might be increased up to the maximum power level according to the regulation which is recommended by FCC, IEEE, or ICNIRP. In this context, FCC regulations restrict the maximum output power level for each frequency band. For instance, the maximum output power level is 4 W EIRP for 900 MHz frequency band. Then, geometric shapes of the transmitting antenna may be enlarged to increase the antenna gain of transmitter if it is possible. As shown in equation (6), the higher the frequency, the higher the attenuation. Therefore, operating at lower frequencies should be preferred for lower attenuation. Broadcasting many RF frequency bands can increase the power density of the environment. Considering that the power density level is inversely proportional to the square of distance, the distance between source and measurement point plays a critical role. For that reason, the closer the harvesting antenna is to the transmitter, the

higher the power density at the surroundings of the harvesting antenna and the higher the power output at the harvesting antenna. Note that, for other than free space environment, the power density level is inversely proportional to the nth power of distance (r^n), where n is a constant value [28]. While the value of n equals 2 for free space environment, the value of n is less than 2 for reflective environment. In case of non-line of sight, the value of n can be higher than 2.

On the other hand, the effective area of the antenna is also important for the received power of the harvesting antenna. In order to achieve the efficiency in air interface, we express the wireless transmission medium output power as the input power of harvesting antenna as

$$P_w = P_t G_t \left(\frac{\lambda}{4\pi r}\right)^2. \tag{7}$$

Finally, we can express the efficiency in air interface by eliminating the impact of harvesting antenna as

$$\eta_{air} = G_t \left(\frac{\lambda}{4\pi r}\right)^2. \tag{8}$$

It can be observed that, the wavelength of transmitted RF signal, i.e., the associated frequency, directly affects the values of power and efficiency. Before the design of an RF energy harvesting system, it should be determined that which frequency band or bands have the high power density levels in the ambient environment. The amount of power harvested depends on the frequencies available. For this reason, various electromagnetic spectral surveys were conducted in different countries [1,10,29–36]. In Ref. [10], in order to determine the power density levels in urban and semi urban areas, an RF spectral survey was conducted between 0.3 and 3 GHz in Greater London in the United Kingdom in 2012. As depicted in Fig. 3, the power density levels of Digital TV, GSM900, GSM1800, UMTS (3G) and Wi-Fi bands were measured. It was determined that the Digital TV, GSM900, GSM1800, UMTS (3G) bands were the most promising bands for the measurements. In Ref. [29], several field measurements were performed by using a spectrum analyzer in indoor and outdoor environments in Covilha, Portugal. Power density levels of 36 different locations were measured and some of these measurements were taken in indoor and outdoor environments. The most suitable frequency bands were GSM900 and GSM1800 bands according to the field measurements. RF energy

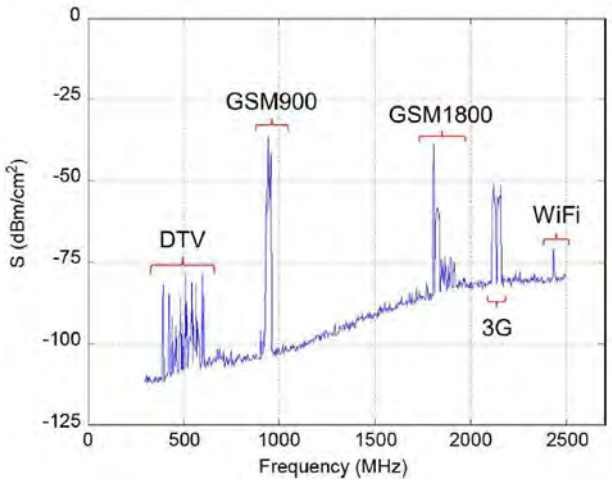

Fig. 3. RF power density levels at measured frequencies in Greater London [10].

harvesting circuit was designed and a dual-band antenna was printed for GSM900 and GSM1800 bands. The gains for the dual band antenna were approximately 1.8 dBi for GSM900 band and 2.06 dBi for GSM1800 band. In Ref. [1], for harvesting RF power, a dual band antenna was designed and implemented. The antenna gains of the dual bands were 1.87 dBi at 915 MHz and 4.18 dBi at 2.45 GHz, respectively. The amounts of the harvested powers were 131.52 μW at 915 MHz and 31.26 μW at 2.45 GHz. On the other hand, measurements of some digital TV bands were performed in the far field in Tokyo, Japan. The height of digital TV antenna was 250 m above ground, and the distance between transmitting antenna and measurement point was 6.3 km. Broadband log periodic antenna (gain of 7 dBi) was used to measure the power level in the environment. While maximum output powers of the Tokyo Metropolitan Television Broadcasting Corporation and the Tokyo Tower bands were 5 kW and 19 kW in the frequency ranges of 512–518 MHz and 560–566 MHz, respectively, the measured power levels were 0.93 μW and 3.73 μW. Moreover, in Ref. [31], a mobile phone operating at 900 MHz was used as a transmitter and the maximum gain of omnidirectional antenna was 1.4 dBi. Maximum transmission power of the mobile phone was 2 W and the measured power level was 1.9 mW at a distance of 2 m from the mobile phone. Where the measured transmitted power levels are low in the far-field region, the proportion of recovered power is low.

3. Antenna and matching circuit

In this section, we discuss the impacts of antenna and matching circuit on the performance of an RF energy harvesting system. We explain antenna, impedance matching circuit, and the efficiency of antenna and matching circuit separately.

3.1. Antenna

Antenna is an essential component in RF energy harvesting systems. Antenna types can be classified according to frequency band, antenna gain, radiation pattern, polarization, physical dimensions or application area, etc. For instance, some antennas can be employed in specific frequency bands such as VHF and UHF. Dipole, loop, array, horn, aperture, microstrip, and log-periodic antennas are some common antenna types. The antenna gain is a measure of conversion from RF signal into electrical signal for a specified direction. In terms of antenna gains, high gain antennas are preferred because they increase the conversion efficiency and directly the amount of harvested energy. Antenna radiation may be isotropic or directional. When a location of an RF signal source (transmitter) is known, a directional antenna can be used to increase the amount of harvested energy. Otherwise, an isotropic antenna can be used. The antenna polarization defines the orientation of electric field at an observation point. If both the transmitting and receiving antennas have the same polarization, the conversion efficiency increases. Horizontal, vertical, circular, and elliptical polarizations are the antenna polarization types.

The physical dimensions of the antenna may vary depending on the power requirements of the circuit for the application. For example, small size antennas are needed in biomedical applications while very large size antennas are used in radio telescopes to observe the celestial objects. Various antenna types are used in airplanes, spacecraft, ships, or cars. Some software design programs such as High Frequency Structure Simulator (HFSS) [37], Advanced Design System (ADS) [38], and Computer Simulation Technology (CST) [39] are tools to design an antenna or other circuit components. Antenna parameters (e.g., gain, directivity, return loss) can be computed and optimized with these programs and then the

appropriate antennas can be fabricated on a printed circuit board (e.g., FR4 that is a flame retardant composite dielectric material).

Total electromagnetic energy in the surroundings of the harvesting antenna is distributed in various spectral bands. A promising frequency band or bands are determined by spectral measurements, as mentioned in the previous section. Based on the measurement results, the design of single band, multiband, or broadband antennas can be suitable to be used in RF energy harvesting systems. Designing and manufacturing of single band antenna is simple but it harvests less energy compared to the multiband antennas [40]. Besides, output DC voltage level of the RF energy harvester is increased if energy harvester circuit is designed for multiple frequency bands [34]. A broadband antenna is proper for harvesting the power from wide frequency band but its antenna gain decreases as away from the center frequency [41]. Furthermore, providing the impedance matching across a wideband is a very challenging task.

Multiple antennas are suitable for harvesting more power [40–45], and this more power may enhance the RF-DC conversion efficiency [42,44,45] but using the multiple antennas lead to the expansion of the circuit size [46] and also increase the cost. In Ref. [40], a triple band modified Yagi-Uda patch antenna was designed, simulated, and fabricated for 900 MHz, 1800 MHz, and 2.45 GHz frequency bands. Measured and simulated results of the reflected coefficients were in good agreements. Antenna gains were 3.26 dBi, 3.02 dBi, and 6.88 dBi for 900 MHz, 1800 MHz, and 2.45 GHz frequency bands, respectively. It was determined that multiband RF energy harvester achieved 15% more conversion efficiency than single band RF energy harvester in this study. The amount of harvested energy can be further increased by utilizing the high gain antennas [47] and polarization matching [48].

Note that the efficiency increases the amount of harvested energy, but the increase in the amount of harvested energy does not necessarily mean an increase in the efficiency. As an example, the amount of harvested energy may be increased by using two identical antennas operating at the same frequency band in an energy harvesting system, but in this case, the efficiency of the system remains the same.

There are many studies about distributed antenna systems in the literature [49–51]. Distributed antenna energy systems surrounding a target area provide efficient energy harvesting. Fig. 4 shows two distributed antennas as a 20-element dual linearly polarized narrowband patch array and a 64-element dual circularly polarized broadband spiral array [52]. The actual size of 20-element dual linearly polarized narrowband patch array is 22 cm × 28 cm and the actual size of 64-element dual circularly polarized broadband spiral array 18.5 cm × 18.5 cm. Operating frequency of distributed antennas are 1.96 GHz and 2–18 GHz, and the array size and amount of harvested power is scalable. The amount of harvested energy can be increased by attaching a conductive reflector to such an antenna array [48]. Through an experiment, the authors demonstrated that the output voltage of two monopole antennas with a conductive reflector was greater than without the reflector.

We also mention about wearable antennas as wearable antennas have attracted more attention for RF energy harvesting in the recent years [54–64]. These antenna types can be embedded in clothes. By means of new generation smart clothes containing mixture of textile and conductive materials, health and sport activities can be monitored. If the porous structure of the textile material and the moisture in the fabric are taken into consideration, the dielectric constant and the loss tangent are influenced by these factors. Furthermore, the dielectric constant and the loss tangent directly affect the antenna performance (i.e., antenna conversion efficiency) [29]. A novel three dimensional textile antenna array was presented in Ref. [64]. The antenna was designed and simulated by HFSS. The antenna patch and ground were made of copper wires and its substrate was made of glass fiber. The measurement results showed that input matching and radiation patterns of the antenna were good but its gain was low. As illustrated in Fig. 5, a wideband planar logarithmic spiral textile antenna was designed [62] by CST Microwave Studio. Operating frequencies and the measured antenna gains were 2.4 GHz, 5 GHz, 8 GHz and −0.12 dBi, 0.2 dBi, −0.63 dBi, respectively. It is seen that antenna gains are low.

Wearable antennas are flexible antennas, and bending of these antennas may degrade the antenna performance [60] and change the resonant frequency [57,65]. In addition, antenna miniaturization is a technique that reduces the antenna size [58,63,66–68], and miniaturization of an antenna dimensions may cause a tradeoff between antenna size and antenna performance. In Ref. [63], miniaturized printed elliptical nested fractal multiband antenna was designed and simulated using ADS for 910 MHz, 2.4 GHz, 3.2 GHz, 5 GHz and fabricated on FR4. Hilbert fractal structures were used to enhance the impedance matching for these frequencies. According to the best knowledge of the authors, it was the widest bandwidth antenna operating from 900 MHz to 6 GHz at that small scale for RF energy harvesting applications. Measured gains of the multiband antennas were −8.4 dBi, 0.74 dBi, 1.4 dBi and 1.6 dBi for 1 GHz, 1.92 GHz, 2.05 GHz and 2.7 GHz, respectively. Simulation and measurement results for antenna gain and return loss were close to each other. In Ref. [54], a circular disk microstrip wearable antenna was designed for 2.4 GHz (Wi-Fi) band. Copper and Flectron electro textile were used for the conductive parts of the antennas separately. In addition to that, in both cases, indigo blue jeans cotton fabrics were preferred for substrate materials. It was simulated that the frequency bandwidth was 116.74 MHz and

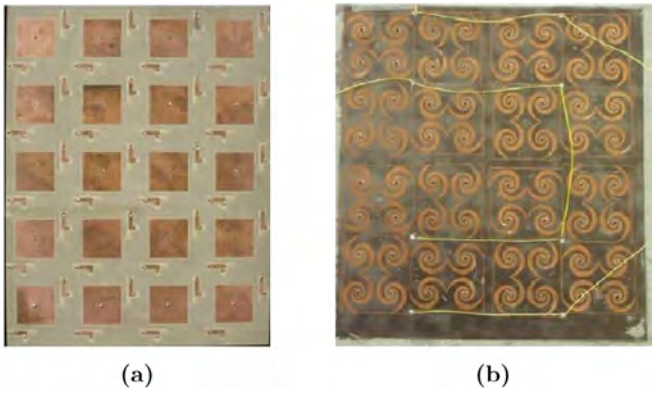

Fig. 4. (a) 20-element dual linearly polarized narrowband patch array (22 cm × 28 cm) and (b) 64-element dual circularly polarized broadband spiral array (18.5 cm × 18.5 cm) [52,53].

Fig. 5. Embroidered textile spiral logarithmic antenna [62].

return loss was −32 dB for the copper case. Whereas the frequency bandwidth was 113.27 MHz and return loss was −23.13 dB for the electro textile case. In terms of the simulation results, the antenna gain and conversion efficiency were 5.75 dBi and 56.12% for the copper case, respectively. Whereas the antenna gain and conversion efficiency were 5.19 dBi and 50% for the electro textile case, respectively. In that study, it may be deduced that the electro textile patch antennas is a good alternative to a solid substrate patch antenna. It is observed that the higher the antenna gain, the higher the antenna conversion efficiency.

3.2. Matching circuit

There are numerous impedance matching studies [22,46,69–72]. Simple matching circuit can be designed from a combination of resistance, inductor or capacitor. The resistor is the real part of the impedance, and the inductor and the capacitor are the reactive parts. Only using resistors for impedance matching causes power loss. In this case, only the real part of the impedance is matched [46]. Quarter-wavelength transformer is a technique that uses a $\lambda/4$ transformer for matching the antenna to the other part of the circuit. If the impedance of the antenna just consists of real part, this transformer is directly connected to the load. However, if the impedance of the antenna consists of both real and reactive parts, the transformer is connected to a proper distance from the antenna [22]. An ideal impedance matching between an antenna and a load can be accomplished by using shunt stub matching depicted in Fig. 6. If ends of the stub are left open-circuit, it is called open-circuited shunt stub. However, if ends of the stub are connected to each other, it is called short-circuited shunt stub. As shown in Fig. 6, the length s is varied to make the real part of the antenna impedance equal to the real part of the line impedance. The length l of the shunt stub is changed to make the susceptance of the stub equal to in magnitude but opposite in phase to the susceptance of the line at the connection point of the antenna and the transmission line.

L type, Π type and T type impedance matching networks are some of impedance matching network topologies as illustrated in Fig. 7. In Ref. [46], all of these impedance matching network topologies were designed for RF energy harvesting circuits. L type impedance matching network generally consists of series capacitor with shunt inductor or vice versa. In Ref. [46], the frequency bandwidth of the Π type impedance matching network is wider than L type but the efficiency of the RF energy harvesting circuit of the L type is more than the Π type. In addition to that, the T type improves the output voltage levels. In Fig. 7, C and L represent capacitor and inductor, respectively. TL represents any circuit element that contains resistance, capacitor or inductance.

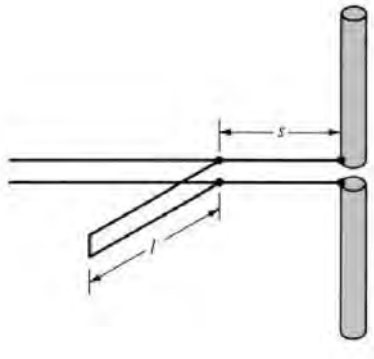

Fig. 6. Shunt stub matching [22].

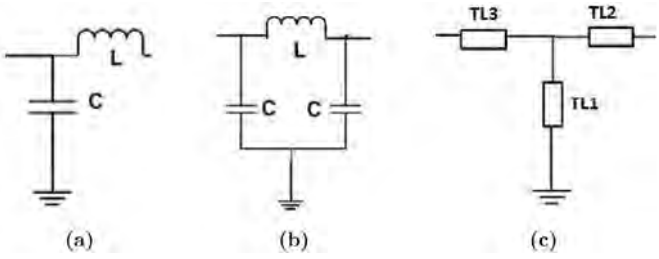

Fig. 7. (a) L type (b) Π type (c) T type impedance matching network topologies [46].

In Ref. [70], an improved dynamic impedance matching network was suggested for maximizing the harvested energy. The inductive part of the antenna was tried to balance by three different capacitors. According to the input power level, the proper capacitor was selected by the control unit. In that study, it was shown that this method was always better than static and no matching method. In Ref. [73], a novel method was applied for eliminating the impedance matching between an antenna and a rectifier. The high input impedance of an off center fed dipole antenna was well match to the high input impedance of a broadband rectifier. Since both the antenna and the rectifier have the same impedance values, the impedance matching circuit between them is not needed.

3.3. Efficiency of antenna and matching circuit

The harvesting antenna of an RF energy harvesting system converts the electric field strength of the incident RF signal into the voltage level at the antenna terminals. Then a matching circuit is used to match the impedances of antenna and rectifier. There are various parameters that affect the efficiency of antenna and matching circuit. It can be formulated as follows

$$\eta_{ant} = \frac{P_a}{P_w}. \tag{9}$$

In addition to that, the efficiency of antenna and matching circuit can also be stated by conversion and impedance matching efficiencies

$$\eta_{ant} = \eta_{con,ant}\ \eta_{im,ant}. \tag{10}$$

This efficiency can be rearranged by the conduction, dielectric, and impedance matching efficiencies,

$$\eta_{ant} = \eta_c \eta_d \eta_{im,ant}, \tag{11}$$

where η_c is the conduction efficiency, η_d is the dielectric efficiency, and $\eta_{im,ant}$ is the impedance matching efficiency [22]. All efficiencies are dimensionless. The conduction and dielectric efficiencies can be combined as

$$\eta_{cd} = \eta_c \eta_d, \tag{12}$$

where η_{cd} is the antenna radiation efficiency, the values of η_c and η_d can be determined experimentally, and they are very difficult to compute [22]. The conduction efficiency and dielectric efficiency are affected by conduction and dielectric losses within the structure of the antenna. So if possible, low conduction and dielectric losses material should be selected for antenna manufacturing. The impedance matching efficiency can be expressed as

$$\eta_{im,ant} = 1 - |\Gamma_{ant}|^2, \tag{13}$$

where Γ_{ant} is the reflection coefficient as a ratio of impedance mismatch. If there is no impedance mismatch in a circuit, it means that there is no reflected power. So there is no power loss in the circuit. The reflection coefficient can be formulated as

$$\Gamma_{ant} = \frac{Z_L - Z_A}{Z_L + Z_A}, \tag{14}$$

where Z_L is the input impedance of the rectifier, and Z_A is the input impedance of the antenna.

When the direction of the incoming wave and the position of the antenna are considered, the polarization loss factor becomes important parameter

$$\mathrm{PLF} = \left|\rho_w \rho_a\right|^2, \tag{15}$$

where PLF is the polarization loss factor, ρ_w is the unit polarization vector of incoming (incident) wave, and ρ_a is the unit polarization vector of electric field strength of the receiving antenna. If both unit polarization vectors are match, the value of PLF would be one. It means that there is no polarization loss.

In this context, the antenna radiation efficiency can also be formulated by the antenna effective area, impedance matching between air and antenna, directivity, and polarization loss factor. Optimization of all these parameters increases the antenna radiation efficiency

$$\eta_{cd} = \frac{A_{eff}}{\left(1 - \left|\Gamma_{air}\right|^2\right) D_0 \frac{\lambda^2}{4\pi} \left|\rho_w \rho_a\right|^2}, \tag{16}$$

where A_{eff} is the antenna effective area, Γ_{air} is the reflection coefficient as a ratio of impedance mismatch between air and antenna, D_0 is the directivity of the antenna.

If there are no impedance mismatch and polarization mismatch, i.e., $\left(1 - \left|\Gamma_{air}\right|^2\right) = 1$ and $\left|\rho_w \rho_a\right|^2 = 1$, the formula of the antenna radiation efficiency can be simplified as follows

$$\eta_{cd} = \frac{A_{eff}}{D_0 \frac{\lambda^2}{4\pi}}. \tag{17}$$

When the output power level of antenna and matching circuit (P_a) and received power level (P_w) are taken into account, the efficiency in antenna and matching circuit block (η_{ant}) is calculated as shown in equation (9). For increasing the efficiency in antenna and matching block, the conversion efficiency $(\eta_{con,ant})$ of antenna should be kept high as much as possible. In addition, if impedances of the antenna and rectifier are matched very well, the impedance matching efficiency of antenna block $(\eta_{im,ant})$ would be the maximum. Therefore, the maximum efficiency will be achieved in the antenna and matching circuit block.

To achieve maximum power transfer between the antenna and the rectifier blocks, the impedance of the antenna should be equal to the complex conjugate of the impedance of the rectifier circuit. Otherwise, power loss occurs and therefore, efficiency drops. Rectifiers generally utilize diodes and other circuit components. Due to the nonlinear nature of diodes, the impedance of the rectifier circuit varies with operating frequency, input power level, and impedance of load [73]. For these reasons, impedance matching circuit for nonlinear components becomes very challenging task. Moreover, the impedance matching is not only required between the antenna and the rectifier blocks, but also between other circuit parts. Therefore, the same impedance matching formula can be applied to the other blocks as well.

4. Rectifier

In this section, we present the effects of rectifier on the performance of an RF energy harvesting system. Numerous studies on rectifiers in energy harvesting system exist in literature [74–82]. Rectifier is a circuit that converts RF or AC power to DC power. The rectifier is a vital part of the RF energy harvesting system, which has a significant impact on the overall efficiency. Input power level, input voltage level, input impedance, output impedance, parasitic effects, and operating frequency are some parameters of the rectifier circuit that must be optimized to enhance the RF-DC power conversion efficiency. Conversion and impedance matching efficiencies of the rectifier circuit are explained in detail.

4.1. Rectification methods

Various rectification methods are used during the RF-DC power conversion. As shown in Fig. 8, half-wave, full-wave, and bridge rectification methods are only some of these methods [74]. V_{peak} represents the peak level of the AC voltage signal. In the half-wave rectification circuit, there is only one diode D1. When the AC voltage signal is applied to the input of the diode D1 in the half-wave of Fig. 8, only the positive voltage cycle passes through and negative part of the voltage cycle is lost. In terms of RF energy harvesting, this method is the simplest method but not suitable for some applications. In the full-wave rectification circuit, there are two diodes D1 and D2 and two capacitors C1 and C2. When the diode D1 conducts the negative voltage cycle and the capacitors C1 is charged up to V_{peak} voltage level, the diode D2 is off. On the other hand, the diode D2 conducts the positive voltage cycle and the capacitor C2 is charged and during this process, the diode D1 is off. Therefore, output voltage (V_{out}) of the full-wave rectification is the twice V_{peak} voltage level over a period. In terms of the RF energy

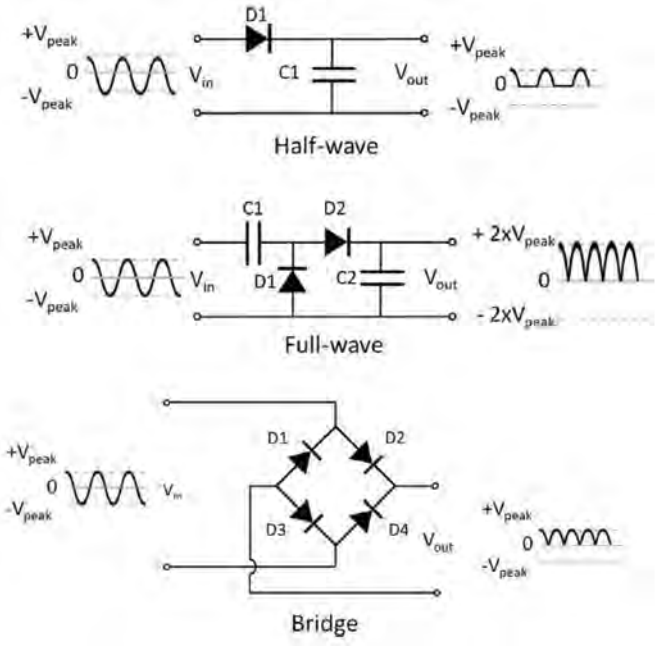

Fig. 8. Half-wave, full-wave and bridge rectification methods [74].

harvesting, the full-wave rectification is more efficient than the half-wave rectification. In the bridge rectification circuit, there are four diodes: D1, D2, D3 and D4. When the diode D2 and D3 conduct the positive voltage cycle over half a period, the diode D1 and D4 are off. Whereas, the diodes D1 and D4 conduct the negative voltage cycle over half a period, the diodes D2 and D3 are off. Thus, the output voltage (V_{out}) of the bridge rectification is at V_{peak} voltage level [74].

4.2. Schottky diodes

A diode is often used as a rectification component. The choice of diode for the rectifier circuits is critical in designing an efficient energy harvesting system. Owing to low forward voltage drop, low power consumption, low parasitic effects, and high switching speed, Schottky diodes are preferred in the rectifier circuits. Some common Schottky diode types and their parameters are illustrated in Table 3 [83,84]. In order to enhance the RF-DC power conversion efficiency and maximize the harvested RF power, the forward voltage drop of the diode is minimized, and input voltage level of the rectifier circuit is increased [14,85]. When the input voltage level of the rectifier circuit is not greater than the forward voltage drop of the diode, the rectifier circuit would not work. Besides, when the reverse breakdown voltage is exceeded, a failure will occur in diode. Due to the nonlinear behavior of the diode, the RF-DC power conversion efficiency varies with input power level of the diode. The increased input power level of the diode improves the RF-DC power conversion efficiency significantly. These issues should be considered when selecting the most suitable diode for the design of the rectifier circuit.

A Schottky barrier diode consists of metal layer, n-type or p-type epitaxial layer and n-type or p-type silicon substrate. Fig. 9 depicts the low frequency equivalent circuit of a Schottky diode [83]. R_S is the parasitic series resistance of a diode, which represents the resultant resistance of bulk layer of silicon substrate, bondwire, leadframe and so on. The RF energy coupled into R_S is dissipated as heat energy. Thus, this dissipated energy degrades the RF-DC power conversion efficiency. Similarly, C_P and L_P exhibit parasitic capacitance and parasitic inductance, respectively. The parasitic components in the rectifier should be kept as low as possible to enhance the RF-DC power conversion efficiency [14]. Cj is the junction capacitance of the Schottky diode and has also parasitic effect. The thickness of epitaxial layer and the diameter of the Schottky diode influence the value of the Cj. R_V is the video junction resistance that depends on the current flowing through the Schottky diode. In general, the p-type and n-type diodes are used for small signal detector and mixer applications, respectively.

For Agilents HSMS-285× family of the Schottky diodes, the values of R_S, C_P, and L_P are 25 Ω, 0.08 pF, and 2 nH, respectively. Cj is 0.18 pF and R_V is 9 kΩ. HSMS-285× family of the Schottky diodes are designed for the input power level less than −20 dBm and the frequency below 1.5 GHz. As another type, HSMS-282× Schottky diode series are designed for the input power level greater than −20 dBm and the frequency below 4 GHz. Similarly, HSMS-286× Schottky diode series are designed for the input power level greater than −20 dBm and the frequency above 4 GHz [83].

Table 3
Schottky diode types.

Schottky Diode Types	Forward Voltage Drop VF (mV)	Reverse Breakdown Voltage VBD (V)
HSMS-2822	340	15
HSMS-2852	150–250	3.8
HSMS-2862	250–350	7
SMS-7630	60–120	2
CDF-7621	270–350	3

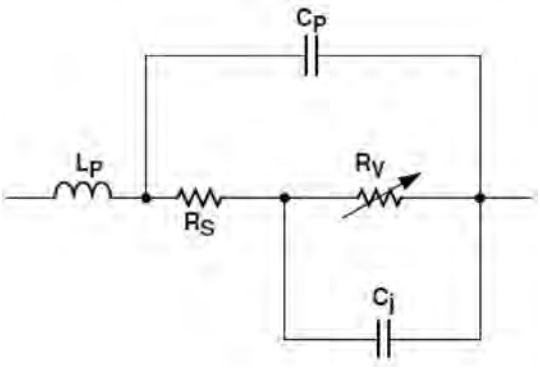

Fig. 9. Low frequency equivalent circuit of a Schottky diode [83].

Note that, with recent technological developments, alternative diode types such as Esaki (tunnel) and Spin diodes have been developed for the Schottky diodes. Due to the low parasitic components, Esaki diodes can be used to operate at very high frequency band. Moreover, Spin diodes provide lower forward voltage drop than the Schottky diodes [74].

4.3. Single/multi band rectifiers

Single band rectifier collects the power in the ambient environment from a single frequency band and it can be suitable for simple energy harvesting system. However, this collected power may be insufficient to operate a device (e.g., a sensor node). For that reason, multiband rectifier is chosen to scavenge more power from different frequency bands simultaneously. In addition, the wideband rectifier may also provide more harvested power. In Ref. [86], a single band operating at GSM850 and a trial band operating at GSM850, GSM1900 and Wi-Fi (2.4 GHz) bands fully gate cross-coupled (FGCC) rectifier was designed and simulated. The trial band rectifier presented the highest power conversion efficiency between 0 and 5 μW input power levels. Besides, it has also better power conversion efficiency than the single band operating at GSM850 rectifier and enhanced the power conversion efficiency by maximum 20% at the same input power range. According to the simulation results, this trial band rectifier achieved the power conversion efficiency of 66.3% at −23.2 dBm input power level per channel with 100 kΩ load resistance. Moreover, this trial band rectifier utilizing low-threshold-voltage (LTV) transistors was also compared to the other published single [14,87,88] and double band rectifiers [89] and it was determined that the trial band rectifier showed a higher power conversion efficiency.

4.4. Input/output impedance

Matching of input and output impedances of the rectifier circuit is a challenging task. Due to the nonlinear nature of the diode, the input impedance of the diode varies with input power level and operating frequency [79]. In order to enhance the efficiency of the rectifier circuit, the variations in input and output impedance of the rectifier circuit should be kept in balance. In other words, the output impedance and the input impedance which is affected by the variation of input power level must be matched. Otherwise, the efficiency of the rectifier circuit drops significantly. Various impedance matching techniques were investigated in Section 3. Apart that, another technique which is called resistance compression network is employed. A resistance compression network is an

impedance matching network [90–94] and it can be located between antenna and rectifier. The resistance compression network is used to minimize the sensitivity of rectifier circuit to the large variation of the input power level of the diode and output impedance of the load. The large variation of the input power level of the diode and the large variation of the output impedance of the load are supported by the small variation of the input impedance of the rectifier circuit and hence, the RF-DC power conversion efficiency is improved. Fig. 10 shows the small variation of the input resistance versus the large variation of the load resistance [91]. In Ref. [90], a dual band rectifier based on the resistance compression network operating at 915 MHz and 2.45 GHz was proposed, designed and implemented. The RF-DC power conversion efficiencies versus the input power levels of the proposed and conventional rectifiers were depicted in Fig. 11. Thanks to the proposed rectifier based on the resistance compression network, the improved RF-DC power conversion efficiency was achieved when compared with a conventional envelope detector.

4.5. Efficiency of rectifier

The efficiency in the rectifier block can be divided into the RF-DC power conversion efficiency and impedance matching efficiency. As illustrated in Fig. 1, when the output power level of the rectifier circuit (P_r) and the output power level of the antenna and matching circuit (P_a) are taken into consideration, the efficiency in the rectifier block (η_{rec}) can be calculated as

$$\eta_{rec} = \frac{P_r}{P_a}, \tag{18}$$

$$\eta_{rec} = \eta_{con,rec}\eta_{im,rec}. \tag{19}$$

As in equation (19), the efficiency of the rectifier block can also be expressed as conversion efficiency ($\eta_{con,rec}$) and impedance matching efficiency of the rectifier block ($\eta_{im,rec}$). If the power loss, parasitic resistance, parasitic capacitance and parasitic inductance which degrade the RF power conversion efficiency in rectifier block are minimized, the RF-DC power conversion efficiency would be maximized. In the same way, if the input and output impedance of the rectifier block circuit are matched, the maximum efficiency would be achieved in the rectifier block.

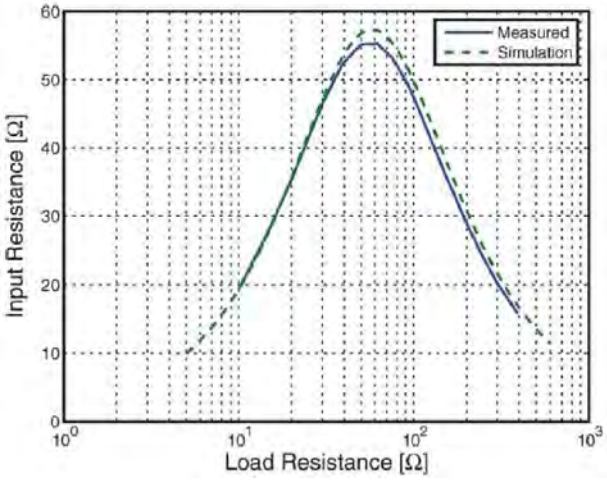

Fig. 10. Input resistance versus load resistance [91].

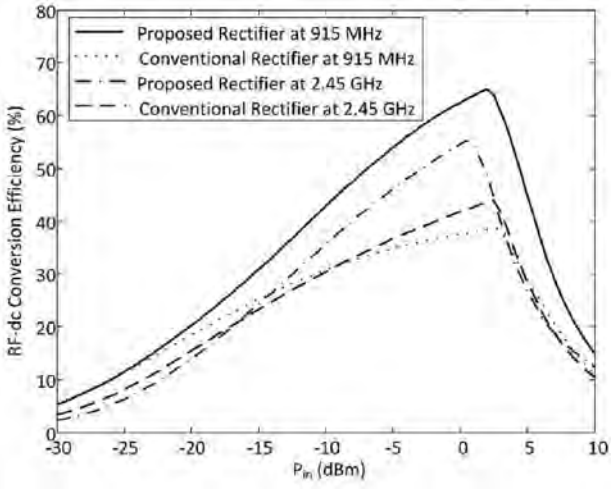

Fig. 11. RF-DC power conversion efficiencies versus the input power levels [95].

5. Voltage multiplier

In this section, we present the impacts of voltage multiplier on the performance of an RF energy harvesting system. The output DC voltage level of the rectifier may be not sufficient to drive a device or sensor. For that reason, a DC-DC voltage converter circuits such as voltage multiplier, charge pumps or voltage booster are used to increase the output DC voltage level of the rectifier.

5.1. Voltage multiplier topologies

Various voltage multiplier topologies exist in literature [35,95–101]. Villard and Dickson voltage multipliers are the most common voltage multipliers in wireless energy harvesting systems. Villard voltage multiplier is also known as Cockcroft-Walton voltage multiplier [101]. As shown in Fig. 12, two stage Cockcroft-Walton and Dickson voltage multipliers consist of diodes and capacitors used as voltage up-converters. Since the high threshold voltage level and the parasitic effects of the diodes degrade the DC-DC power conversion efficiency, the selection of the proper diode is very crucial for obtaining maximum power conversion efficiency. Each voltage multiplier stage consists of two capacitors and diodes. In Dickson voltage multiplier topology, parallel capacitors are used to feed diodes while series capacitors are used in Cockcroft-Walton voltage multiplier topology [100]. The larger capacitor stores more energy but it takes more time to charge [101]. Due to the parallel configuration of the capacitors, more stages increase the total capacitance of the Dickson voltage multiplier. So it just increases the reactive part of the impedance. In addition to that, the output voltage of the Dickson voltage multiplier depends on the number of stages

$$V_{out} = 2n\left(V_{in} - V_{fwd}\right), \tag{20}$$

where n is the number of voltage multiplier stages, V_{in} is the input voltage level, and V_{fwd} is the forward voltage drop. V_{out} is the output voltage level with no load. As seen in equation (20), V_{out} is directly proportional to the number of voltage multiplier stages [29]. Practically, parasitic effects and leakage currents of the diodes and capacitors restrict the number of voltage multiplier stages. Thus, they limit the DC-DC power conversion efficiency and voltage gain.

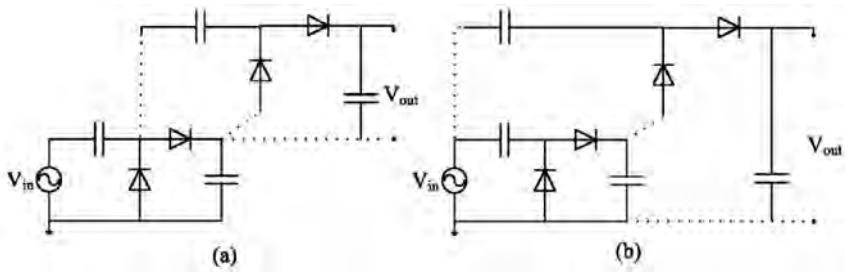

Fig. 12. (a) Cockcroft-Walton voltage multiplier (b) Dickson voltage multiplier [29].

5.2. Voltage multiplier stages

The number of voltage multiplier stages is a critical parameter for RF energy harvesting, which should be determined optimally to obtain the maximum value of DC-DC power conversion efficiency. If there are few voltage multiplier stages, the output DC voltage level of the voltage multiplier may be insufficient to drive a wireless device. As the number of voltage multiplier stage increases, the output DC voltage level and the voltage gain of the voltage multiplier increase up to the optimal point. However, if the number of voltage multiplier stages exceeds this optimal point, it leads to a decrease in output DC voltage level and voltage gain. For this reason, the number of voltage multiplier stages should be at the optimal point for the maximum DC-DC power conversion efficiency. Moreover, as the number of voltage multiplier stages increases, the peak of power conversion efficiency moves towards the higher power value. Fig. 13 depicts the effect of the number of stages on the power conversion efficiency [97]. The peak of power conversion efficiency shifts from the lower power to the higher power region while the number of voltage multiplier stages increases. So the operation of the large number of voltage multiplier stages in the low power level environment may reduce the power conversion efficiency.

In Ref. [102], it was shown that the DC-DC power conversion efficiency of the voltage multiplier was dependent on the input power level. The input power and output power levels of the voltage multiplier were −13 dBm and −20 dBm, respectively, while the incident RF power level of the antenna was −5 dBm. The DC-DC power conversion efficiency of the voltage multiplier was approximately 19%. Besides, the input power and output power levels of the voltage multiplier were −5.1 dBm and −6.7 dBm, respectively, while incident RF power of the antenna was 0 dBm. In this case, the DC-DC power conversion efficiency of the voltage multiplier was approximately 69%. It was observed that the DC-DC power conversion efficiency was also enhanced when the input power level was increased up to an optimal point.

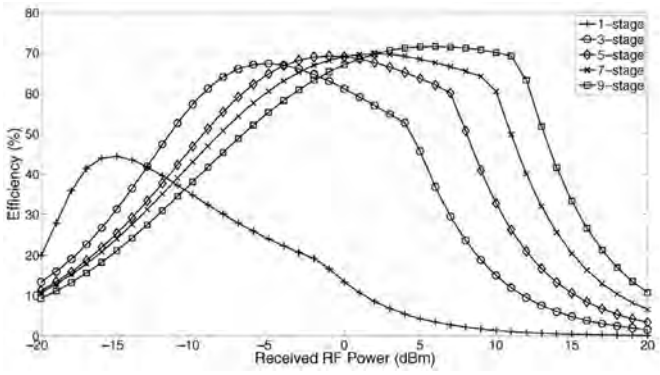

Fig. 13. Effect of the number of stages on the power conversion efficiency of voltage multiplier [97].

5.3. Designing by CMOS technology

Voltage multipliers and rectifiers can also be designed by Complementary Metal Oxide Semiconductor (CMOS) technology [87,103–108]. CMOS technology utilizes both NMOS and PMOS transistors. Fig. 14 depicts the four stage Dickson voltage multiplier [74]. Owing to the CMOS technology, designed voltage multipliers may be more sensitive than customary Schottky diodes at low voltage levels. In order to obtain higher power conversion efficiency and voltage gain, various existing voltage multiplier circuits were modified [103–106]. The lower threshold voltage of the CMOS process is more sensitive but allows more leakage current, which causes a power loss and degrades the overall efficiency [74]. So there is a tradeoff between threshold voltage and leakage current.

Owing to channel resistance and gate capacitance, the impedance of the MOS transistor divides into resistive and capacitive components [109]. Various voltage multiplier or rectifier stages can be cascaded. Cascading multiple voltage multiplier stage in series causes capacitors to be connected in series and resistors to be connected in parallel [14]. In that way, the total resistive component decreases as the total capacitive component increases. If the total resistive component drops too low, the parasitic resistance of the circuit starts to affect the system and degrades the power conversion efficiency. In addition to that, there is a relationship between the size of transistor and the parasitic capacitance [110]. So the parasitic capacitance increases as the size of the transistor increases. On the other hand, if the size of the transistor is reduced, it will allow less current to flow. Furthermore, a decrease in channel width causes an increase in channel resistance of the transistor. In addition, as the operating frequency increases, the parasitic effects also increase. All of these will affect the circuit performance. Therefore, an optimum size of transistor and operating frequency should be chosen in voltage multiplier circuit design.

In terms of multiple stage voltage multiplier or rectifier designs, it is very important to achieve the highest possible power conversion efficiency. Besides, its input power range should be as wide as possible. In this way, power conversion efficiency is kept high level, and more amount of harvested energy is obtained at the same time. In Ref. [111], Fig. 15 shows the power conversion efficiency across

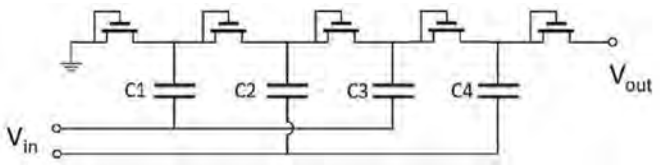

Fig. 14. Four stage Dickson voltage multiplier based on CMOS technology [74].

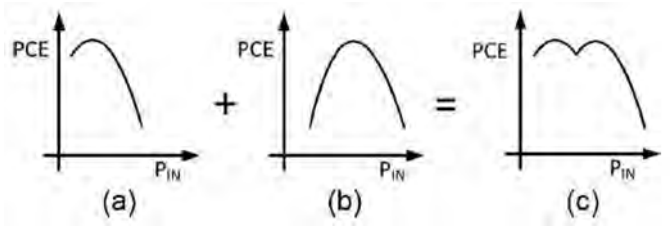

Fig. 15. (a) Power conversion efficiency versus low input power level (b) Power conversion efficiency versus high input power level (c) Power conversion efficiency versus extended input power range [111].

the several input power levels. A dual path rectifier circuit operating at 900 MHz was designed for both a low input power path and a high input power path. For this purpose, the circuit was manufactured in a 65-nm CMOS technology with input power range from −16 dBm to −5 dBm. According to the input power levels, the adaptive control circuit selected the best path for achieving the high power conversion efficiency across the extended power range. Thereby, the dual path energy harvester maintained approximately 20% power conversion efficiency with 11 dB input power ranges while single path energy harvester only maintained high power conversion efficiency with 8 dB input power ranges [111].

5.4. Efficiency of voltage multiplier

The efficiency in the voltage multiplier block can be divided into the DC-DC power conversion efficiency and impedance matching efficiency. As depicted in Fig. 1, when the output power level of the voltage multiplier circuit (P_m) and the output power level of the rectifier circuit (P_r) are taken into account, the efficiency in the voltage multiplier block (η_{mul}) can be calculated as

$$\eta_{mul} = \frac{P_m}{P_r}, \tag{21}$$

$$\eta_{mul} = \eta_{con,mul}\eta_{im,mul}. \tag{22}$$

As seen in equation (22), the efficiency of the voltage multiplier block can also be stated as conversion efficiency ($\eta_{con,mul}$) and impedance matching efficiency ($\eta_{im,mul}$). If the power losses and parasitic effects in voltage multiplier circuit are minimized, the DC-DC power conversion efficiency would be maximized. At the same time, if the input and output impedances of the voltage multiplier circuit are matched, the maximum efficiency would be achieved in the voltage multiplier block.

6. Energy storage or load

Energy harvesting circuits are designed to produce a certain amount of power. If the average harvested power is greater than the power consumption of the load (e.g., device or sensor), the energy harvesting circuit may feed the load continuously [112]. Therefore, no energy storage device is required. Otherwise, the harvested power should be stored in an energy storage device. The impedance of the energy harvesting circuit depends on various parameters such as input power level, operating frequency, load impedance, rectifier or voltage multiplier topologies, etc. Maximum power transfer can only be obtained when the load impedance is well matched to the circuit. For this reason, there is an optimum load impedance for each input power level and operating frequency. As seen in Fig. 16, the highest RF-DC power conversion efficiency was achieved only at certain load resistances [100], while the input

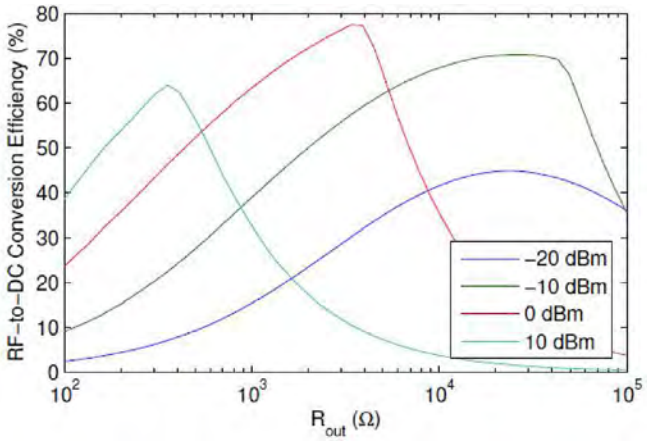

Fig. 16. RF-DC power conversion efficiency versus load resistance [100].

power levels were different. If these certain load resistance value is too high or too low, the RF-DC power conversion efficiency greatly degrades. So the energy harvesting circuit should be designed by choosing the optimum load to achieve the highest power conversion efficiency. The energy storage devices can be considered as a load for the energy harvesting systems. The performances of energy storage devices are compared by using the Ragone plot, where energy density is plotted versus power density [113]. Note that the energy density represents the amount of energy per mass (Wh/kg) and the power density represents the amount of power per mass (W/kg) in the Ragone plot. Hence, the Ragone plot shows the time required to deliver the energy in the energy storage devices comparatively. In RF energy harvesting systems, supercapacitors or rechargeable batteries can be used to store the harvested energy.

6.1. Supercapacitors

Supercapacitors are electrochemical double layer capacitors with high energy storage capacity. They have higher power density than batteries and higher energy density than conventional capacitors. Because of these features, supercapacitors are placed between the conventional capacitors and the batteries. Owing to quick charging times, good discharge performance and long lifetime, the supercapacitors are preferred to accumulate the harvested energy [29]. A supercapacitor can be modeled by an ideal capacitor and an internal resistance. The capacity value of supercapacitor drops to 80%, and the internal resistance value doubles in 10 years [114]. With decreasing capacities, the actual life of supercapacitors can be up to 20 years. The efficiency of supercapacitors is dependent on the charging and discharging efficiencies. Considering a supercapacitor as a load in the energy harvesting circuit, the charging efficiency decreases with the increase in the value of internal resistance. The charging efficiency of supercapacitor is sufficiently high because of low internal resistance. The internal resistance of supercapacitor with 350 F capacity is measured in mΩ levels [115]. However, the high self-discharge feature degrades the efficiency of supercapacitor, which causes a decrease in the efficiency of the energy harvesting system.

6.2. Batteries

Batteries are an energy storage alternative of supercapacitors, which can also be utilized as rechargeable power supply in the energy harvesting circuits. There are various type batteries such as nickel cadmium (NiCd), sealed lead acid (SLA), nickel metal hydride

(NiMH), lithium (Li), and Lithium ion (Li-ion). Lithium and lithium alloy batteries are more advantageous than other batteries because they are more efficient. The equivalent model of a battery can be shown as a series connection of an ideal voltage source and an internal resistance [116]. Considering a battery as a load in the energy harvesting circuit, the charging efficiency of battery changes with the charging current. There is an optimum point for the charging current to maximize the charging efficiency of battery [117]. Batteries have higher energy density than supercapacitors as well as conventional capacitors, as an advantage. However, batteries have lower power density and lower lifetime than supercapacitor, as disadvantages. In addition to that, new energy storage device that is called supercapattery has been developed recently. Supercapatteries have carbon nanotubes and redox materials as an electrode, which combine the best advantage parts of supercapacitors and batteries [118]. A supercapattery has higher energy storage capacity value than supercapacitors and quicker charge and discharge value than batteries. Because of these advantages, it will contribute to the efficiency of energy harvesting systems.

In an energy harvesting system, the type of energy storage device should be decided on the basis of advantages and disadvantages, such as energy density, power density, leakage current, lifetime, size, charging and discharging efficiencies.

6.3. Efficiency of energy storage device or load

The efficiency in the energy storage device or load block is directly related with the impedance of the block. The impedance matching efficiency of the energy storage device or load block can be calculated as

$$\eta_{im,load} = 1 - |\Gamma_{load}|^2. \tag{23}$$

Γ_{load} is the reflection coefficient and a ratio of impedance mismatch between load and voltage multiplier circuit as

$$\Gamma_{load} = \frac{Z_{load} - Z_{mul}}{Z_{load} + Z_{mul}}, \tag{24}$$

where Z_{load} is the input impedance of the load and Z_{mul} is the input impedance of the voltage multiplier circuit. While there is no impedance mismatch between load and voltage multiplier circuit, there is no reflected power and the reflection coefficient would be zero. Thus, there is no power loss in the circuit.

7. Power management

Power management can be regarded as a common process involving rectifier, voltage multiplier, and energy storage units. In this context, it affects the efficiency of all these units. Power management is a smart application to maximize the efficiency and harvested energy in wireless energy harvesting system. For these reasons, Power Management Unit (PMU) is utilized in many energy harvesting circuits [1,10,52,99,119,120]. Fig. 17 illustrates the PMU placed in the energy harvesting circuit [121]. Power management can be provided by Maximum Power Point Tracking (MPPT), which is applied to energy sources with time-varying power. The MPPT aims to obtain maximum power from the energy source by adjusting current or voltage based on the current-voltage curve of the energy source [122]. A MPPT algorithm is used to find the optimal point for the maximum generated power [123] and this algorithm runs under the PMU application. Moreover, the MPPT algorithm can be executed by different techniques. The PMU allows the wireless energy harvesting circuit to monitor the harvested energy levels and provides the charge control and charge protection of the energy storage devices such as capacitors or batteries [52]. Thanks to the PMU, the efficiency of the energy harvesting system can be tracked and optimized.

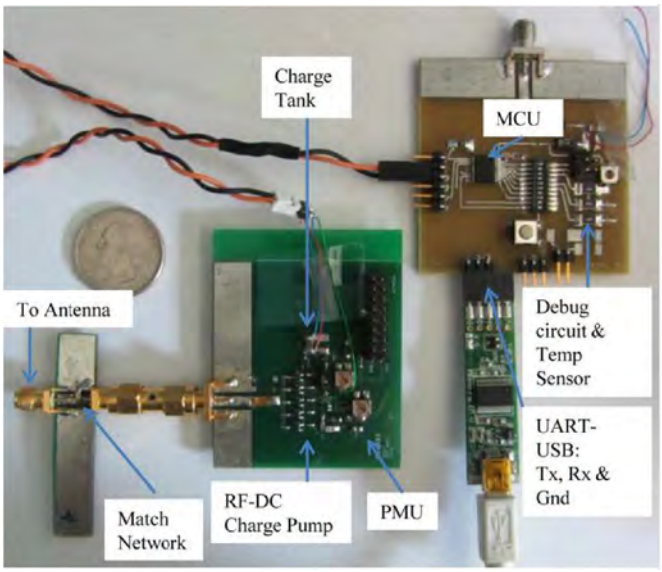

Fig. 17. PMU in the energy harvesting circuit [121].

In Ref. [99], an optimized PMU was designed to enhance the efficiency of DC-DC power converter. The inductor value, fitness function and on-time were optimized parameters for the DC-DC power converter efficiency. The resistor emulation and particle swarm optimization techniques were utilized to determine the optimum parameter values. The resistor emulation technique was used to follow the maximum power point at low power levels. On the other hand, the purpose of the particle swarm optimization technique was to find the best values of inductor and on-time which provide the maximum efficiency. In this study, it was determined that the efficiency of the optimized PMU was 9.25% more than conventional PMU. In Ref. [124], a power management circuit is implemented for RF energy harvesting, which 87.7% efficiency is achieved for 2.4 μW power. In Ref. [125], a microcontroller-based power management system is designed for RF energy harvesting, and the amount of harvested energy is significantly improved by means of MPPT and adaptive optimization algorithm. Thus, with power management, it is possible to enhance the efficiency of wireless energy harvesting systems. The efficiency provided by the PMU can be considered in the efficiency of rectifier, voltage multiplier, and energy storage units.

8. Efficiency of energy harvesting circuit

The efficiency is one of the most important features that show the performance of an energy harvesting circuit. It directly affects the amount of energy obtained from the energy harvesting circuit. Therefore, the efficiency of the energy harvesting circuit should be increased as much as possible. Energy harvesting circuit mainly consists of antenna and matching circuit, rectifier, voltage multiplier and energy storage device or load blocks. The efficiency in the energy harvesting circuit can be expressed as seen equation in (25) and (26). In terms of conversion efficiency and impedance matching efficiency, this formula can be extended as depicted in equation (27). The efficiency of wireless transmission medium (η_{air}) is not included in the energy harvesting circuit but it is included in the energy harvesting system. However, the efficiency of the wireless transmission medium is explained in detail in the previous

subsection (efficiency of wireless transmission medium subsection). Hence, it can be written

$$\eta_{ehc} = \frac{P_a}{P_w}\frac{P_r}{P_a}\frac{P_m}{P_r}\frac{P_s}{P_m}, \quad (25)$$

$$\eta_{ehc} = \eta_{ant}\,\eta_{rec}\,\eta_{mul}\,\eta_{load}, \quad (26)$$

$$\eta_{ehc} = \eta_{con,ant}\eta_{im,ant}\,\eta_{con,rec}\eta_{im,rec}\,\eta_{con,mul}\eta_{im,mul}\,\eta_{im,load}, \quad (27)$$

where η_{ehc} is the efficiency of energy harvesting circuit.

In order to obtain the maximum efficiency, each block in the energy harvesting circuit must be optimized. The impedance matching between the blocks must be achieved for obtaining the maximum impedance matching efficiency in each block. On the other hand, the conduction efficiency and dielectric efficiency should be increased by reducing the conduction and dielectric losses within the antenna structure for maximum conversion efficiency in the antenna and matching circuit block. In this way, the conversion efficiency in the antenna and matching circuit block is improved. For obtaining the maximum conversion efficiency in rectifier block, the power loss, parasitic resistance, parasitic capacitance, and parasitic inductance should be decreased as much as possible. Likewise, the power losses and parasitic effects in voltage multiplier block should be minimized for achieving the maximum conversion efficiency in the voltage multiplier circuit. Finally, the energy harvesting circuit should be terminated with the most appropriate load value.

There are many designed and implemented wireless energy harvesting circuits in the literature [43,90,126–138]. In terms of efficiency, some implemented RF energy harvesting circuits which the maximum power conversion efficiency is greater than 50% and a few less than 50% were investigated in detail in Table 4. In addition to that, two studies were included, which indicate lower power conversion efficiencies. The related articles were sorted by frequency bands. Within each frequency band, the maximum power conversion efficiencies were ordered from the largest to the smallest, respectively. For that reason, some relevant articles were selected and investigated in terms of maximum efficiency, frequency band, antenna gain, diode type, load, etc.

In Ref. [126], a high efficiency wireless energy harvesting circuit was designed and implemented for 2.45 GHz. The measured gain of the two element dipole array microstrip antenna was 8.6 dBi. The Schottky HSMS-2852 diode was shunted across the antenna which was designed to match the circuit. The maximum power conversion efficiency of 83% was achieved while the input power level was approximately 0 dBm and the load was 1400 Ω.

In Ref. [127], a dual input rectifier was designed and fabricated for 2.45 GHz. This rectifier was connected to the two ports of dual linearly polarized patch antenna which can receive all polarization of incident wave. Horizontal and vertical gains of the antenna were 7.45 dBi (H) and 7.63 dBi (V), respectively. The Schottky HSMS-2860 diode was connected to the circuit as a single shunt diode. The maximum power conversion efficiency of 78% was obtained while the input power density was 295.3 $\mu W/cm^2$ and the load was 550 Ω.

In Ref. [128], an enhanced differentially driven rectifier was proposed. Differentially fed microstrip patch antenna was designed and manufactured for 2.45 GHz. The measured antenna gain is 5.47 dBi. The Schottky HSMS-2860 diodes were used for differentially driven rectifier topology. The maximum power conversion efficiency of 73.9% was achieved for a rectifier with an antenna while the input power level was 10.4 dBm and the load was 1400 Ω.

In Ref. [129], a rectifier and an antenna were presented as a rectenna for wireless energy harvesting circuit. The rectifiers topology was the two stage Dickson voltage multiplier utilizing the HSMS-2852 diodes. Koch fractal patch antenna gain was 4 dBi and

Table 4
Conversion efficiency.

Ref.	Frequency (GHz)	Band	Conversion Efficiency (%)	Input Power (dBm)	Output Voltage (V)	Antenna Type	Antenna Gain (dBi)	Antenna Dim. (mm)	Topology	Load (Ω)	Diode Type
[126]	2.45	Single	83	0	1	Microstrip	8.6	80 × 87	Shunt diode	1400	HSMS-2852
[127]	2.45	Single	78	295.3 $\mu W/cm^2$		Patch	7.45 (H) 7.63 (V)	70 × 70	Shunt diode	550	HSMS-2860
[128]	2.45	Single	73.9	10.4		Patch	5.47	70 × 100	Diff. driven	1400	HSMS-2860
[129]	2.45	Single	70	3	1.6	Patch	4		Dickson multiplier	13000	HSMS-2852
[130]	2.45	Dual	66.8	10	2.6	Just rectifier no antenna			Series diode	1050	HSMS-2860
	5.8		51.5	10	2.3						
[90]	0.915	Dual	65	0		Just rectifier no antenna			Series diode	1000	SMS-7630
	2.45		55	0							
[131]	0.85	Dual	15	−20		Patch			Series diode	2200	SMS-7630
	1.85		15								
[132]	0.5–1.0	Triple	55	27		Just rectifier no antenna			Series diode	50	HSMS-282×
	1.5–2.0										
	2.3–3.6										
[133]	0.9	Triple	45	−15		Patch	3.26	170 × 48	Dickson multiplier	50000	HSMS-2852
	1.8		46				3.02				
	2.45		25				6.88				
[43]	0.876–0.959	Quad	84	5.8	0.9	Dipole	6	100 × 100	Voltage doubler	11000	MSS20-141
	1.71–1.88										
	1.92–2.17										
	2.41–2.48										
[134]	0.6–1.15	Broad	80.1	39.03		Just rectifier no antenna			Class-F	34	
[135]	0.9–1.1	Broad	75	20		Dipole	1.8		Shunt diode	250–3000	HSMS-2820
	1.8–2.5						3.5				
							3.3				
[136]	0.9–2.45	Broad	50	−3	2.1	Patch	6	50 × 50	Series diode	2400	HSMS-2850
			68	14	1.45				Shunt diode	750	HSMS-2860
			78	23	4.2				Bridge rectifier	200	HSMS-2820
[137]	0.47–0.86	Broad	60	10		Just rectifier no antenna			Dickson multiplier	12200	SMS-7630
[138]	1.8–2.5	Broad	55	−10		Dipole	2.5–4.12	70 × 70	Bridge rectifier	14700	SMS-7630

designed for 2.45 GHz. The advantage of this type antenna was its overall size and bandwidth. The maximum power conversion efficiency of 70% was achieved for rectenna while the input power level was approximately 3 dBm and the load was 13 kΩ. The implemented rectenna was able to harvest enough power to operate the 1.6 V light emitting diode from the 3.1 m far away the transmitter.

In Ref. [130], a dual band rectifier was realized for 2.45 GHz and 5.8 GHz. There is no antenna in this circuit. For maximum power transfer, a dual band impedance matching circuit was implanted. The Schottky HSMS-2860 diode was used as a single series diode. When the input power level was 10 dBm and the load was 1050 Ω, the maximum power conversion efficiencies were 66.8% and 51.5% for 2.45 GHz and 5.8 GHz, respectively. In addition to that, the peak DC voltages were 2.6 V for 2.45 GHz and 2.3 V for 5.8 GHz.

In Ref. [90], a dual band rectifier operating at 0.915 GHz and 2.45 GHz was presented. There is no antenna design in this circuit. A dual band resistance compression networks were utilized for impedance matching circuit and also used to reduce the sensitivity of input power and output load variation. Thus, improved power conversion efficiency was obtained when it is compared to traditional envelope detector. The Schottky SMS-7630 diode was used as a single series diode. When the input power level was 0 dBm and the load was 1 kΩ, the maximum power conversion efficiencies were over 65% and 55% for 0.915 GHz and 2.45 GHz, respectively.

In Ref. [131], a dual band rectenna operating at 0.85 GHz and 1.85 GHz was presented. Broadband monopole patch antenna was fabricated for dual band. The Schottky SMS-7630 diode was used as a single series diode. When the input power level was −20 dBm and the load was 2.2 kΩ, the maximum power conversion efficiency was 15% for both 0.85 GHz and 1.85 GHz.

In Ref. [132], a triple band rectifier which covers the wide frequency band was designed and fabricated for 0.5–1.0 GHz, 1.5–2.0 GHz, and 2.3–3.6 GHz. There is no antenna design in this circuit. The Schottky HSMS-282× diode was used as a single series diode for rectifier topology. A composite right left handed transmission line technique was utilized to form a multi band antenna. The maximum power conversion efficiency of 55% was achieved while the input power level was 27 dBm and the load was 50 Ω.

In Ref. [133], a triple band rectifier which covers the wide frequency range was designed for 0.9 GHz, 1.8 GHz, and 2.45 GHz. The Schottky HSMS-2852 diodes were chosen for Dickson voltage multiplier. Modified Yagi-Uda patch antenna was fabricated for triple band. The antenna gains were 3.26 dBi (0.9 GHz), 3.02 dBi (1.8 GHz) and 6.88 dBi (2.45 GHz). When the input power level was −15 dBm and the load was 50 kΩ, the maximum power conversion efficiencies were 45% for 0.9 GHz and 46% for 1.8 GHz and 25% for 2.45 GHz, respectively.

In Ref. [43], a quad band rectenna covering GSM900, GSM1800, UMTS and Wi-Fi frequency bands was designed and fabricated for wireless energy harvesting. The high gain of wideband dipole antenna receiving the frequency band from 0.9 GHz to 3 GHz was 6 dBi. The Schottky MSS20-141 diodes were chosen for modified voltage doubler topology. In this circuit, impedance matching network was realized for maximum power transfer. In order to operate the energy harvesting circuit, the minimum input power level was −20 dBm. The maximum power conversion efficiency of 84% was obtained while the input power level was 5.8 dBm and the load was 11 kΩ. At −15 dBm, DC output voltage level was 0.9 V.

In Ref. [134], a broadband class F-1 rectifier was realized for ranging from 0.6 GHz to 1.15 GHz. There is no antenna design. Input and output impedance matching circuits were used in this circuit. The maximum power conversion efficiency of 80.1% was achieved while the input power level was 39.03 dBm (8 W) and the load was 34 Ω.

In Ref. [135], a broadband high efficiency rectifier covering 0.9–1.1 GHz and 1.8–2.5 GHz was designed and fabricated. In this design, broadband off-center-fed dipole antenna was chosen for high input impedance. The input impedance of this antenna was directly matched to the input impedance of the rectifier. Therefore, impedance matching network was eliminated. The gains of broadband off-center-fed dipole antenna were 1.8 dBi for 0.9 GHz, 3.5 dBi for 1.8 GHz, and 3.3 dBi for 2.4 GHz. Various diodes such as SMS-7630, HSMS-2850, HSMS-2860, and HSMS-2820 were used to achieve maximum efficiency. The peak efficiency was obtained using HSMS-2820 diode as a shunt diode. The maximum power conversion efficiency of 75% was achieved while the input power level was 20 dBm and the load was between 250 Ω and 3000 Ω.

In Ref. [136], three different rectenna topologies were designed and implemented for ranging from 900 MHz to 2.45 GHz. In the first rectenna architecture, the Schottky HSMS-2850 diode was used as a series mounted diode for low input power level which was below 0 dBm. In the second rectenna architecture, the Schottky HSMS-2860 diode was utilized as a shunt mounted diode for medium input power level which was between 0 dBm and 20 dBm. In the third rectenna architecture, the Schottky HSMS-2820 diode was used as a bridge diode for high input power level which was above 20 dBm. WLAN patch antenna was utilized for all rectifier topologies. The gain of the WLAN patch antenna was 6 dBi. According to the input power level, the appropriate rectenna (rectifier and antenna) was activated for energy harvesting by power management system. The maximum power conversion efficiency of 50% was achieved for series mounted diode rectenna while the input power level was −3 dBm and the optimum load was 2.4 kΩ. Furthermore, the maximum power conversion efficiency of 68% was obtained for shunt mounted diode rectenna while the input power level was 14 dBm, and the optimum load was 750 Ω. Finally, the maximum power conversion efficiency of 70% was achieved for bridge diode rectenna while the input power level was 20 dBm and the optimum load was 200 Ω. For the first, second, and third rectennas, the DC output voltage levels were 2.1 V at 0 dBm, 1.45 V at 10 dBm, and 4.2 V at 20 dBm, respectively.

In Ref. [137], a broadband rectifier was designed and manufactured for ranging from 470 MHz to 860 MHz. In this design, there is no antenna. An impedance matching circuit based on a non-uniform transmission line was utilized for impedance matching in this circuit. The Schottky SMS-7630 diodes were chosen for two stage Dickson voltage multiplier. The maximum power conversion efficiency of 60% was achieved while the input power level was 10 dBm and the load was 12.2 kΩ.

In Ref. [138], a novel broadband rectenna ranging from 1.8 GHz to 2.5 GHz was designed and fabricated for wireless energy harvesting. Dual polarized cross dipole was used to improve the receiving capability in this circuit. The gains of dual polarized cross dipole antenna were 2.5 dB for 1.8 GHz and 4.2 dB for 2.5 GHz. A novel impedance matching network was based on two different branches to improve the rectenna efficiency. The Schottky SMS-7630 diodes were used for a two stage voltage doubler circuit. The minimum input power level was down to −35 dBm. The maximum power conversion efficiency of 55% was achieved while the input power level was −10 dBm and the optimum load was 14.7 kΩ.

9. Conclusion

RF energy signals are ubiquitous and they have vital advantages for RF energy harvesting systems. Compared to the other energy sources such as solar, thermal gradients and mechanical vibrations,

the power density of RF energy is relatively low but the amount of harvested energy is sufficient to power up some sensors or devices. In this study, not only theoretical knowledge but also practical application areas were highlighted. An RF energy harvesting system has been thoroughly reviewed in this paper. The blocks of an RF energy harvesting circuit, which are antenna and matching circuit, rectifier, voltage multiplier, and energy storage device or load blocks, have been investigated based on efficiency in detail. Antenna types and gains, impedance matching techniques, diode types, multiplier stages, supercapacitors, batteries and loads were explained separately. In order to obtain the maximum efficiency, optimization of each block in the energy harvesting circuit was discussed so that all the parameters affecting the efficiency were explained. Furthermore, some designed and implemented energy harvesting circuits were presented and investigated. In the light of aforementioned information, it is seen that the performance of an RF energy harvesting system depends on many factors such as transmit power, propagation distance, frequency band, operation voltage, antenna gain, antenna number, matching topology, rectification method, diode type, voltage multiplier topology, multiplier stage number, power management algorithm, energy storage device type, and load impedance. This paper has provided a basis for efficiency in RF energy harvesting that is a promising technology for future research. RF energy harvesting technology, which allows devices to acquire their own energies, is attracting much interest. The design of the various components required to collect and store or use the energy directly is becoming well developed. It is expected that this technology will continue to grow and improve well beyond the current status we have been able to show in this paper.

References

[1] Kim Sangkil, Vyas Rushi, Jo Bito, Niotaki Kyriaki, Collado Ana, Georgiadis Apostolos, Manos M, Tentzeris. Ambient RF energy-harvesting technologies for self-sustainable standalone wireless sensor platforms. Proc IEEE 2014;102(11):1649–66.
[2] Jaffe Paul, McSpadden James. Energy conversion and transmission modules for space solar power. Proc IEEE 2013;101(6):1424–37.
[3] Green Martin A, Emery Keith, Hishikawa Yoshihiro, Warta Wilhelm, Dunlop Ewan D. Solar cell efficiency tables (Version 38). Prog Photovoltaics Res Appl 2011;19(5):565–72.
[4] Siddique Abu Raihan Mohammad, Rabari Ronil, Mahmud Shohel, Van Heyst Bill. Thermal energy harvesting from the human body using flexible thermoelectric generator (fteg) fabricated by a dispenser printing technique. Energy 2016;115:1081–91.
[5] Leonov Vladimir. Thermoelectric energy harvesting of human body heat for wearable sensors. IEEE Sens J 2013;13(6):2284–91.
[6] Turkmen Anil Can, Celik Cenk. Energy harvesting with the piezoelectric material integrated shoe. Energy 2018;150:556–64.
[7] Orecchini G, Yang L, Tentzeris MM, Roselli L. Wearable battery-free active paper printed RFID tag with human-energy scavenger. IEEE MTT-S International Microwave Symposium Digest 2011:2–5.
[8] Kim Heung Soo, Kim Joo Hyong, Kim Jaehwan. A review of piezoelectric energy harvesting based on vibration. Int J Precis Eng Manuf 2011;12(6):1129–41.
[9] Yildiz Faruk. Potential ambient energy-harvesting sources and techniques. J Technol Stud 2009;35(1).
[10] Piñuela Manuel, Mitcheson Paul D, Lucyszyn Stepan. Ambient RF energy harvesting in urban and semi-urban environments. IEEE Trans Microw Theory Tech 2013;61(7):2715–26.
[11] Bi Suzhi, Ho Chin Keong, Zhang Rui. Wireless powered communication: opportunities and challenges. IEEE Commun Mag 2015;53(4):117–25.
[12] Ng DWK, Lo ES, Schober R. Wireless information and power transfer: energy efficiency optimization in OFDMA systems. IEEE Trans Wirel Commun 2013;12(12):6352–70.
[13] Takacs A, Okba A, Aubert H, Charlot S, Calmon P-F. Recent advances in electromagnetic energy harvesting and wireless power transfer for IoT and shm applications. IEEE International Workshop of Electronics, Control, Measurement, Signals and their Application to Mechatronics 2017:1–4.
[14] Triet Le, Mayaram Karti, Fiez Terri. Efficient far-field radio frequency energy harvesting for passively powered sensor networks. IEEE J Solid State Circuits 2008;43(5):1287–302.
[15] Reinisch Hannes, Gruber Stefan, Hartwig Unterassinger, Wiessflecker Martin, Hofer Gnter, Pribyl Wolfgang, Holweg Gerald. An electro-magnetic energy harvesting system with 190 nW idle mode power consumption for a BAW based wireless sensor node. IEEE J Solid State Circuits 2011;46(7):1728–41.
[16] Powercast. P2110 - 915 MHz RF Powerharvester receiver data sheet. 2018. http://www.powercastco.com.
[17] Guha Koushik. RF energy harvesting in agriculture. In: 8th all India peoples technology congress; 2011. p. 1–5.
[18] Jo Bito, Kim Sangkil, Tentzeris Manos, Nikolaou Symeon. Ambient energy harvesting from 2-way talk-radio signals for smart meter and display applications. IEEE Antennas and Propagation Society International Symposium 2014:1353–4.
[19] Radiofrequency Electromagnetic Fields. Evaluating compliance with fcc guidelines for human exposure to radiofrequency electromagnetic fields. OET Bulletin 1997;65(10).
[20] IEEE. Standard for safety levels with respect to human exposure to radio frequency electromagnetic fields, 3 kHz to 300 GHz. IEEE Std C95 2005:1–238. 1-2005.
[21] ICNIRP. Guidelines for limiting exposure to time-varying electric, magnetic, and electromagnetic fields (up to 300 GHz). Health Phys 1998;74(4):494–522.
[22] Balanis CA. Antenna theory: analysis and design. third ed. John Wiley & Sons; 2005.
[23] Pinuela Manuel, Yates David C, Lucyszyn Stepan, Mitcheson Paul D. Maximizing DC-to-load efficiency for inductive power transfer. IEEE Trans Power Electron 2013;28(5):2437–47.
[24] Kurs A, Karalis A, Moffatt R, Joannopoulos JD, Fisher P, Soljacic M. Wireless power transfer via strongly coupled magnetic resonances. Science 2007;(5834):83–6.
[25] Jiang B, Smith JR, Philipose M, Roy S, Sundara-Rajan K, Mamishev AV. Energy scavenging for inductively coupled passive RFID systems. IEEE Transactions on Instrumentation and Measurement 2007;56(1):118–25.
[26] Finkenzeller Klaus. RFID handbook: fundamentals and applications in contactless smart cards, radio frequency identification and near-field communication. John Wiley & Sons; 2010.
[27] Shoki Hiroki. Issues and initiatives for practical deployment of wireless power transfer technologies in Japan. Proc IEEE 2013;101(6):1312–20.
[28] Rappaport Theodore S. Wireless communications: principles and practice. New Jersey: Prentice Hall PTR; 1996.
[29] Barroca Norberto, Saraiva Henrique M, Gouveia Paulo T, Tavares Jorge, Luis M, Borges Fernando J Velez. Caroline loss, rita salvado, pedro pinho, ricardo goncalves, nuno BorgesCarvalho, raul chavez-santiago, and ilangko balasingham. Antennas and circuits for ambient RF energy harvesting in wireless body area networks. IEEE 24th Annual International Symposium on Personal, Indoor, and Mobile Radio Communications 2013:532–7.
[30] Cansiz Mustafa, Abbasov Teymuraz, Bahattin Kurt Muhammed, Celik Ali Recai. Mobile measurement of radiofrequency electromagnetic field exposure level and statistical analysis. Measurement: Journal of the International Measurement Confederation 2016;86:159–64.
[31] Pascal Ancey. Ambient functionality in MIMOSA from technology to services. In: Proceedings of the 2005 joint conference on Smart objects and ambient intelligence innovative context-aware services: usages and technologies. New York, USA: ACM Press; 2005. p. 35.
[32] Kawahara Yoshihiro, Tsukada Keisuke, Asami Tohru. Feasibility and potential application of power scavenging from environmental RF signals. IEEE Antennas and Propagation Society, AP-S International Symposium (Digest) 2009;I:3–6.
[33] Cansiz Mustafa, Abbasov Teymuraz, Kurt M Bahattin, Recai Celik A. Mapping of radio frequency electromagnetic field exposure levels in outdoor environment and comparing with reference levels for general public health. J Expo Sci Environ Epidemiol 2016:1–5.
[34] Sun Hucheng, Guo Yong-xin, He Miao, Zheng Zhong. A dual-band rectenna using broadband Yagi antenna array for ambient RF power harvesting. IEEE Antennas Wirel Propag Lett 2013;12:918–21.
[35] Arrawatia Mahima, Baghini Maryam Shojaei, Kumar Girish. RF energy harvesting system from cell towers in 900MHz band. In: IEEE national conference on communications; 2011. p. 1–5.
[36] Noguchi Akira, Arai Hiroyuki. Small loop rectenna for RF energy harvesting. In: IEEE asia-pacific Microwave conference proceedings; 2013. p. 86–8.
[37] HFSS. High Frequency Structure Simulator. 2018. http://www.ansys.com.
[38] ADS. Advanced Design System. 2018. http://www.keysight.com.
[39] CST. Computer Simulator Technology. 2018. http://www.cst.com.
[40] Keyrouz S, Visser Hj, Tijhuis Ag. Multi-band simultaneous radio frequency energy harvesting. Antennas and Propagation 2013:3058–61.
[41] Ali Mai, Albasha Lutfi, Qaddoumi Nasser. RF energy harvesting for autonomous wireless sensor networks. In: 8th international conference on design & technology of integrated systems in nanoscale era; 2013. p. 78–81.
[42] AbdelTawab Ahmed M, Ahmed Khattab. Efficient multi-band energy harvesting circuit for wireless sensor nodes. In: IEEE 4th international Japan-Egypt conference on electronics, communications and computers; 2016. p. 75–8.
[43] Kuhn Veronique, Lahuec Cyril, Seguin Fabrice, Person Christian. A multi-band stacked RF energy harvester with RF-to-DC efficiency up to 84%. IEEE Trans Microw Theory Tech 2015;63(5):1768–78.
[44] Liu Zhongtao, Zheng Zhong, Guo Yong-xin. Enhanced dual-band ambient RF energy harvesting with ultra-wide power range. IEEE Microw Wirel Compon Lett 2015;25(9):630–2.
[45] Agrawal Sachin, Parihar Manoj S, Kondekar PN. A dual-band RF energy

harvesting circuit using 4th order dual-band matching network. Cogent Engineering 2017;4(1):1–10.
[46] Agrawal Sachin, Pandey Sunil Kumar, Singh Jawar, Manoj S, Parihar. Realization of efficient RF energy harvesting circuits employing different matching technique. In: IEEE 15th international symposium on quality electronic design; 2014. p. 754–61.
[47] Agrawal Sachin, Gupta Ravi Dutt, Singh Parihar Manoj, Kondekar Praveen Neminath. A wideband high gain dielectric resonator antenna for RF energy harvesting application. Int J Electron Commun 2017;78:24–31.
[48] Al-Khayari A, Al-Khayari H, Al-Nabhani S, Bait-Suwailam MM, Nadir Z. Design of an enhanced RF energy harvesting system for wireless sensors. In: IEEE 7th GCC conference and exhibition; 2013. p. 479–82.
[49] Choi KaeWon, Ginting Lorenz, Setiawan Dedi, Abdul Aziz Arif, Kim Dong In. Coverage probability of distributed wireless power transfer system. In: IEEE 9th international conference on ubiquitous and future networks; 2017. p. 691–6.
[50] Ng Derrick Wing Kwan, Schober Robert. Secure and green SWIPT in distributed antenna networks with limited backhaul capacity. IEEE Trans Wirel Commun 2015;14(9):5082–97.
[51] Lee Seunghyun, Liu Liang, Zhang Rui. Collaborative wireless energy and information transfer in interference channel. IEEE Trans Wirel Commun 2015;14(1):545–57.
[52] Popovi Zoya, Korhummel Sean, Student Member, Dunbar Steven, Scheeler Robert, Dolgov Arseny, Zane Regan, Member Senior. Scalable RF energy harvesting 2014;62(4):1046–56.
[53] Hagerty JA, Helmbrecht FB, McCalpin WH, Zane Regan, Popovic ZB. Recycling ambient microwave energy with broad-band rectenna arrays. IEEE Trans Microw Theory Tech 2004;52(3):1014–24.
[54] Sankaralingam S, Gupta Bhaskar. A circular disk microstrip WLAN antenna for wearable applications. In: Annual IEEE India conference; 2009. p. 1–4.
[55] Paul Dominique L, Paterson Michael G, Hilton Geoffrey S. A low-profile textile antenna for reception of digital television and wireless communications. In: IEEE radio and wireless symposium; 2012. p. 51–4.
[56] Yang L, Martin L, Staiculescu D, Wong CP, Tentzeris MM. Design and development of compact conformal RFID antennas utilizing novel flexible magnetic composite materials for wearable RF and biomedical applications. In: IEEE antennas and propagation society international symposium; 2008. p. 1–4.
[57] Carter Jason, Saberin Jason, Shah Tejal, Sai Ananthanarayanan PR, Furse Cynthia. Inexpensive fabric antenna for off-body wireless sensor communication. In: IEEE antennas and propagation society international symposium; 2010. p. 1–4.
[58] Park Jung-Yong, Woo Jong-Myung. Microstrip line monopole antenna for the wearable applications. In: IEEE 38th european Microwave conference; 2008. p. 1277–9.
[59] Ito Koichi, Haga Nozomi. Basic characteristics of wearable antennas for body-centric wireless communications. In: IEEE antennas and propagation conference; 2010. p. 42–7.
[60] Kaivanto Emmi K, Berg Markus, Salonen Erkki, de Maagt Peter. Wearable circularly polarized antenna for personal satellite communication and navigation. IEEE Trans Antennas Propag 2011;59(12):4490–6.
[61] Monti Giuseppina, Corchia Laura, Tarricone Luciano. UHF wearable rectenna on textile materials. IEEE Trans Antennas Propag 2013;61(7):3869–73.
[62] Galoic Andrej, Ivsic Branimir, Bonefacic Davor, Bartolic Juraj. Wearable energy harvesting using wideband textile antennas. In: IEEE 10th european conference on antennas and propagation; 2016. p. 1–5.
[63] Albasha Lutfi, Ali Mai, Taghadosi Mansour, Qaddoumi Nasser. Miniaturised printed elliptical nested fractal multiband antenna for energy harvesting applications. IET Microw, Antennas Propag 2015;9(10):1045–53.
[64] Du Cheng-Zhu, Zhong Shun-Shi, Yao Lan, Qiu Yi-Ping. Textile microstrip array antenna on three-dimensional orthogonal woven composite. Proceedings of the 4th European Conference on Antennas and Propagation 2010:4–5.
[65] Kellomaki Tiiti, Heikkinen Jouko, Kivikoski Markku. Effects of bending GPS antennas. In: IEEE asia-pacific Microwave conference, vol. 3; 2006. p. 1597–600.
[66] Rothwell Edward J, Ouedraogo Raoul O. Antenna miniaturization: definitions, concepts, and a review with emphasis on metamaterials. J Electromagn Waves Appl 2014;28(17):2089–123.
[67] Kuga Nobuhiro, Arai Hiroyuki. Circular patch antennas miniaturized by shorting posts. Electron Commun Jpn Part I Commun 1996;79(6):51–8.
[68] Gianvittorio JP, Rahmat-Samii Yahya. Fractal antennas: a novel antenna miniaturization technique, and applications. IEEE Antennas Propag Mag 2002;44(1):20–36.
[69] Hameed Zohaib, Moez Kambiz. Design of impedance matching circuits for RF energy harvesting systems. Microelectron J 2017;62:49–56. Feb.
[70] Felini C, Merenda M, Della Corte FG. Dynamic impedance matching network for RF energy harvesting systems. IEEE RFID Technology and Applications Conference 2014:86–90.
[71] Merz Christian, Kupris Gerald, Harvesting A Energy. High Q impedance matching for RF energy harvesting applications. In: 3rd IEEE international symposium on wireless systems within the conferences on intelligent data acquisition and advanced computing systems; 2016. p. 45–50. Sep.
[72] Adam Ismahayati, Fareq Abd Malek Mohd, Yasin Mohd Najib Mohd, Hasliza A. Rahim. RF energy harvesting with efficient matching technique for low power level application. ARPN Journal of Engineering and Applied Sciences 2015;10(18):8318–21.
[73] Song Chaoyun, Huang Yi, Zhou Jiafeng, Carter Paul, Yuan Sheng, Xu Qian, Fei Zhouxiang. Matching network elimination in broadband rectennas for high-efficiency wireless power transfer and energy harvesting. IEEE Trans Ind Electron 2017;64(5):3950–61.
[74] Tran Le-Giang, Cha Hyouk-Kyu, Park Woo-Tae. RF power harvesting: a review on designing methodologies and applications. Micro and Nano Systems Letters 2017;5(1):14.
[75] Rosli MA, Murad SAZ, Ismail RC. A 900-2400 MHz AC-DC rectifier circuit for radio frequency energy harvesting. MATEC Web of Conferences 2016;78:01096.
[76] Nimo Antwi, Tobias Beckedahl, Ostertag Thomas, Reindl Leonhard. Analysis of passive RF-DC power rectification and harvesting wireless RF energy for micro-watt sensors. AIMS Energy 2015;3(2):184–200.
[77] Yaldi IRH, Rahim SKA, Ramli MR. Compact rectifier design for RF energy harvesting. 2016. p. 11–3. Dec.
[78] Nakura Toru, Matsui Hiroaki, Asada Kunihiro. Comparative study of RF energy harvesting rectifiers and proposal of output voltage universal curves for design guidline. IEICE Electron Express 2015;12(3). 20141114–20141114.
[79] Straughn Matt H, Chen Chi-Chih. Efficient RF energy harvesting circuitry study. In: IEEE 10th european conference on antennas and propagation; 2016. p. 1–4.
[80] Chaour Issam, Ahmed Fakhfakh, Kanoun Olfa. Enhanced passive RF-DC converter circuit efficiency for low RF energy harvesting. Sensors 2017;17(3):546.
[81] Khansalee Ekkaphol, Zhao Yan, Nuanyai Kittipong. High frequency rectifier for RF energy harvesting systems. In: IEEE 7th international conference on information technology and electrical engineering; 2015. p. 304–8.
[82] Collado A, Daskalakis S, Niotaki K, Martinez R, Bolos F, Georgiadis A. Rectifier design challenges for RF wireless power transfer and energy harvesting systems. Radioengineering 2017;26(2):411–7.
[83] Agilent. HSMS-282x, HSMS-285x, and HSMS-286x surface mount Schottky diodes data sheets. 2018. http://www.alldatasheet.com.
[84] Skyworks. CDB, CDC, CDF, and SM76xx series Schottky diodes data sheets. 2018. http://www.skyworksinc.com.
[85] Arai Hiroyuki, Chomora Mikeka, Yoshida Minoru. A voltage-boosting antenna for RF energy harvesting 4 S. 2012. p. 169–72.
[86] Wang Y, Sawan M. High-efficiency CMOS rectifier dedicated for multi-band ambient RF energy harvesting. In: IEEE 21st international conference on electronics, circuits and systems, vol. 2; 2014. p. 179–82.
[87] Papotto Giuseppe, Carrara Francesco, Palmisano Giuseppe. A 90-nm CMOS threshold-compensated RF energy harvester. IEEE J Solid State Circuits 2011;46(9):1985–97.
[88] Umeda T, Yoshida H, Sekine S, Fujita Y, Suzuki T, Otaka S. A 950-MHz rectifier circuit for sensor network tags with 10-m distance. IEEE J Solid State Circuits 2006;41(1):35–41.
[89] Li Bo, Shao Xi, Shahshahan Negin, Goldsman Neil, Salter Thomas, George M, Metze. An antenna co-design dual band rf energy harvester. IEEE Transactions on Circuits and Systems I: Regular Papers 2013;60(12):3256–66.
[90] Niotaki Kyriaki, Georgiadis Apostolos, Collado Ana, John S, Vardakas. Dual-band resistance compression networks for improved rectifier performance. IEEE Trans Microw Theory Tech 2014;62(12):3512–21.
[91] Han Yehui, Leitermann Olivia, Jackson David A, Rivas Juan M, Perreault David J. Resistance compression networks for radio-frequency power conversion. IEEE Trans Power Electron 2007;22(1):41–53.
[92] Xu Junfeng, Tai Wei, Ricketts David S. A transmission line based resistance compression network (TRCN) for microwave applications. IEEE MTT-S International Microwave Symposium Digest 2013:1–3.
[93] Inam Wardah, Afridi Khurram K, Perreault David J. High efficiency resonant DC/DC converter utilizing a resistance compression network. IEEE Trans Power Electron 2014;29(8):4126–35.
[94] Barton Taylor W, Gordonson Joshua M, Perreault David J. Transmission line resistance compression networks and applications to wireless power transfer. IEEE Journal of Emerging and Selected Topics in Power Electronics 2015;3(1):252–60.
[95] Cockcroft JD, Walton ETS. Experiments with high velocity positive ions. Proc Math Phys Eng Sci 1930;129(811):477–89.
[96] Dickson JF. On-chip high-voltage generation in MNOS integrated circuits using an improved voltage multiplier technique. IEEE J Solid State Circuits 1976;11(3):374–8.
[97] Nintanavongsa Prusayon, Student Member, Muncuk Ufuk, Lewis David Richard. Design optimization and implementation for RF energy harvesting circuits design optimization and implementation for RF energy harvesting circuits 2016;2(Feb):24–33.
[98] Devi Kavuri Kasi Annapurna, Din Norashidah Md, Chakrabarty Chandan Kumar. Optimization of the voltage doubler stages in an RF-DC convertor module for energy harvesting. Circuits Syst 2012;03(03):216–22.
[99] Ababneh Majdi M, Perez Samuel, Thomas Sylvia. Optimized power management circuit for RF energy harvesting system. In: IEEE 18th wireless and Microwave technology conference; 2017. p. 1–4.
[100] Marshall Blake R, Morys Marcin M, Durgin Gregory D. Parametric analysis and design guidelines of RF-to-DC Dickson charge pumps for RFID energy harvesting. In: IEEE international conference on RFID; 2015. p. 32–9.
[101] Hamid Jabbar, Song Young S, Jeong Ted Taikyeong. RF energy harvesting

system and circuits for charging of mobile devices. IEEE Trans Consum Electron 2010;56(1):247–53.
[102] Visser Hubregt J, Vullers Ruud JM. RF energy harvesting and transport for wireless sensor network applications: principles and requirements. Proc IEEE 2013;101(6):1410–23.
[103] Wang Weiyin, Chen Xiangjie, Wong Hei. Analysis and design of CMOS full-wave rectifying charge pump for RF energy harvesting applications. In: TENCON IEEE region 10 conference; 2015. p. 1–4.
[104] Dean Karolak, Taris Thierry, Deval Yann, Begueret Jean-Baptiste, Mariano Andre. Design comparison of low-power rectifiers dedicated to RF energy harvesting. In: IEEE international conference on electronics, circuits, and systems; 2012. p. 524–7.
[105] Haddad P-A, Gosset G, Raskin J-P, Flandre D. Efficient ultra low power rectification at 13.56 MHz for a 10 μA load current. In: IEEE SOI-3D-Subthreshold microelectronics technology unified conference; 2014. p. 1–2.
[106] Hameed Zohaib, Moez Kambiz. Hybrid forward and backward threshold-compensated RF-DC power converter for RF energy harvesting. IEEE Journal on Emerging and Selected Topics in Circuits and Systems 2014;4(3):335–43.
[107] Gosset Geoffroy, Flandre Denis. Fully-automated and portable design methodology for optimal sizing of energy-efficient CMOS voltage rectifiers. IEEE Journal on Emerging and Selected Topics in Circuits and Systems 2011;1(2):141–9.
[108] Singh Chouhan Shailesh, Nurmi Marko, Halonen Kari. Efficiency enhanced voltage multiplier circuit for RF energy harvesting. Microelectron J 2016;48:95–102.
[109] Razavi Behzad. Design of analog CMOS integrated circuits. 2001.
[110] Barnett R, Lazar S, Jin Liu. Design of multistage rectifiers with low-cost impedance matching for passive RFID tags. In: IEEE radio frequency integrated circuits symposium; 2006. p. 257–60.
[111] Lu Yan, Dai Haojuan, Huang Mo, Law Man Kay, Weng Sin Sai, Seng-Pan U, Rui P, Martins. A wide input range dual-path CMOS rectifier for RF energy harvesting. IEEE Transactions on Circuits and Systems II: Express Briefs 2017;64(2):166–70.
[112] Harb Adnan. Energy harvesting: state-of-the-art. Renew Energy 2011;36(10):2641–54.
[113] González Ander, Goikolea Eider, Andoni Barrena Jon, Mysyk Roman. Review on supercapacitors: technologies and materials. Renew Sustain Energy Rev 2016;58:1189–206.
[114] Simjee Farhan I, Chou Pai H. Efficient charging of supercapacitors for extended lifetime of wireless sensor nodes. IEEE Trans Power Electron 2008;23(3):1526–36.
[115] Grama A, Petreus D, Borza P, Grama L. Experimental determination of equivalent series resistance of a supercapacitor. In: 32nd international spring seminar on electronics technology; 2009. p. 1–4.
[116] Bhat Rajshekhar Vishweshwar, Motani Mehul, Lim Teng Joon. Energy harvesting communication using finite-capacity batteries with internal resistance. IEEE Trans Wirel Commun 2017;16(5):2822–34.
[117] Krieger Elena M, Arnold Craig B. Effects of undercharge and internal loss on the rate dependence of battery charge storage efficiency. J Power Sources 2012;210:286–91.
[118] Chen George Z. Supercapacitor and supercapattery as emerging electrochemical energy stores. Int Mater Rev 2017;62(4):173–202.
[119] Jung Minchae, Jang Youngrok, Choi Sooyong. Optimal power control for wireless power transfer system: a deterministic approach. In: 2017 ninth international conference on ubiquitous and future networks; 2017. p. 193–6.
[120] Kansal Aman, Hsu Jason, Zahedi Sadaf, Srivastava Mani B. Power management in energy harvesting sensor networks. ACM Trans Embed Comput Syst 2007;6(4):32.
[121] Vyas Rushi J, Cook Benjamin B, Kawahara Yoshihiro, Manos M, Tentzeris E-WEHP. A batteryless embedded sensor-platform wirelessly powered from ambient digital-TV signals. IEEE Trans Microw Theory Tech 2013;61(6):2491–505.
[122] Kansal Aman, Hsu Jason, Srivastava Mani, Raghunathan Vijay. Harvesting aware power management for sensor networks. In: Proceedings of the 43rd annual design automation conference. ACM; 2006. p. 651–6.
[123] Akbari S, Thang PC, Veselov DS. Maximum power point tracking for optimizing energy harvesting process. IOP Conf Ser Mater Sci Eng 2016;151(1):012032.
[124] Saini G, Sarkar S, Arrawatia M, Baghini MS. Efficient power management circuit for RF energy harvesting with 74.27% efficiency at 623nW available power. In: IEEE 14th international new circuits and systems conference; 2016. p. 1–4.
[125] Dolgov Arseny, Zane Regan, Popovic Zoya. Power management system for online low power RF energy harvesting optimization. IEEE Transactions on Circuits and Systems I: Regular Papers 2010;57(7):1802–11.
[126] Sun Hucheng, Guo Yong Xin, He Miao, Zheng Zhong. Design of a high-efficiency 2.45-GHz rectenna for low-input-power energy harvesting. IEEE Antennas Wirel Propag Lett 2012;11:929–32.
[127] Sun Hucheng, Wen Geyi. A new rectenna with all-polarization-receiving capability for wireless power transmission. IEEE Antennas Wirel Propag Lett 2016;15:814–7.
[128] Sun Hucheng. An enhanced rectenna using differentially-fed rectifier for wireless power transmission. IEEE Antennas Wirel Propag Lett 2016;15:32–5.
[129] Olgun Ugur, Chen Chi Chih, John L, Volakis. Wireless power harvesting with planar rectennas for 2.45 GHz RFIDs. In: Symposium digest - 20th URSI international symposium on electromagnetic theory; 2010. p. 329–31.
[130] Wang Defu, Negra Renato. Design of a dual-band rectifier for wireless power transmission. IEEE Wireless Power Transfer 2013:127–30.
[131] Collado Ana, Georgiadis Apostolos. Conformal hybrid solar and electromagnetic (EM) energy harvesting rectenna. IEEE Trans Circuits Syst 2013;60(8):2225–34.
[132] Oka T, Ogata T, Saito K, Tanaka S. Triple-band single-diode microwave rectifier using CRLH transmission line. In: Asia-pacific Microwave conference,(c); 2014. p. 1013–5.
[133] Keyrouz S, Visser HJ, Tijhuis AG. Multi-band simultaneous radio frequency energy harvesting. In: IEEE 7th european conference on antennas and propagation; 2013. p. 3058–61.
[134] Abbasian Sadegh, Johnson Thomas. High efficiency gan hemt synchronous rectifier with an octave bandwidth for wireless power applications. In: IEEE MTT-S international Microwave symposium; 2016. p. 1–4.
[135] Song Chaoyun, Huang Yi, Carter Paul, Yuan Sheng, Xu Qian, Fei Zhouxiang. Matching network elimination in broadband rectennas for high-efficiency wireless power transfer and energy harvesting. In: IEEE Transactions on Industrial Electronics. vol. 64; 2017. p. 3950–61. May.
[136] Marian Vlad, Allard Bruno, Vollaire Christian, Verdier Jacques. Strategy for microwave energy harvesting from ambient field or a feeding source. IEEE Trans Power Electron 2012;27(11):4481–91.
[137] Bolos Ferran, Belo Daniel, Georgiadis Apostolos. A UHF rectifier with one octave bandwidth based on a non-uniform transmission line. In: IEEE MTT-S international Microwave symposium; 2016. p. 1–3.
[138] Song Chaoyun, Huang Yi, Zhou Jiafeng, Zhang Jingwei, Yuan Sheng, Carter Paul. A high-efficiency broadband rectenna for ambient wireless energy harvesting. In: IEEE Transactions on Antennas and Propagation. vol. 63; 2015. p. 3486–95. May.